Springer Series in Optical Sciences 147

Characterization of Partially Polarized Light Fields

Bearbeitet von
Rosario Martínez-Herrero, Pedro M. Mejías, Gemma Piquero

1. Auflage 2012. Taschenbuch. xiii, 179 S. Paperback
ISBN 978 3 642 26028 5
Format (B x L): 15,5 x 23,5 cm
Gewicht: 314 g

Chapter 2
Second-Order Overall Characterization of Non-uniformly Polarized Light Beams

2.1 Introduction

In the previous chapter, the light fields were represented in the space-time domain by means of the BCP matrix (or through the mutual coherence function in the scalar case). For convenience, we will now prefer to work in the space-frequency regime. Consequently, as is well known in the Optics textbooks (Born and Wolf, 1999; Mandel and Wolf, 1995; Perina, 1971; Wolf, 2007) the partially coherent scalar field would then be described (up to second-order) by the so-called cross-spectral density (CSD) $W(\boldsymbol{r}_1, \boldsymbol{r}_2, z; \omega)$, defined in the form

$$W(\boldsymbol{r}_1,\boldsymbol{r}_2,z;\omega) = \overline{E^*(\boldsymbol{r}_1,z;\omega)\, E(\boldsymbol{r}_2,z;\omega)}, \tag{2.1}$$

where E denotes the wide-sense stationary random field, $\boldsymbol{r}_1$ and $\boldsymbol{r}_2$ represent two points at the beam cross-section, orthogonal to the propagation direction z, and the overbar symbolizes the average over the ensemble of realizations. For the sake of simplicity, the explicit dependence on the angular frequency ω of the light beam will be omitted from now on. Although W enables us to propagate analytically the field through optical systems, the accurate experimental determination of the CSD function is not a simple task, and becomes especially difficult for multimode laser beams (for example, those emitted by high-power lasers).

Instead of such a local analysis, there are many situations in which a global characterization would be of more practical use. More specifically, in the present chapter, we are interested in a description of the spatial structure of light fields by means of overall parameters that

(i) are valid for arbitrary beams,
(ii) are defined analytically in a rigorous way,
(iii) are measurable,
(iv) propagate through common optical systems according to simple laws.

Thus, this chapter is arranged as follows. In the next section the overall scalar formalism is shown, and, in Sect. 2.3, a generalization to the vectorial case (i.e., to

R. Martínez-Herrero et al., *Characterization of Partially Polarized Light Fields*, Springer Series in Optical Sciences 147, DOI 10.1007/978-3-642-01327-0_2,

partially polarized beams) is provided. The generalized degree of polarization of non-uniformly polarized fields is introduced in Sect. 2.4. Section 2.5 is devoted to the so-called beam quality parameter of a light field, which provides a meaningful joint description of the focusing capabilities of the beam at the near- and far-field. Application of the above parameters to the particular but important case of partially-polarized Gauss Schell-model beams is analyzed in Sect. 2.6. The possibility of beam quality improvement is considered in Sect. 2.7, and the changes generated on this parameter by different types of optical phase devices are described in Sect. 2.8. Finally, an introductory example of global beam shaping of non-uniformly polarized fields is briefly discussed in Sect. 2.9.

2.2 Second-Order Overall Characterization: Scalar Case

We next provide a survey of the key spatial global characteristics that are commonly used in the scalar framework. They are based on the so-called irradiance moments of the field, which describe the overall spatial structure of the beam. It should be remarked that these scalar parameters and figures of merit have been accepted as current ISO standards for light fields (ISO, 1999, 2003, 2005). Furthermore, the scalar treatment constitutes an appropriate starting point to investigate, in subsequent sections, the polarization behavior in the more involved vectorial case.

2.2.1 Formalism and Key Definitions

To begin with, let us first define the Wigner distribution function (WDF), which is associated to the CSD function through a Fourier transform relationship (Bastiaans, 1989):

$$h(\boldsymbol{r},\boldsymbol{\eta},z) = \int_{-\infty}^{+\infty} W(\boldsymbol{r},\boldsymbol{s},z) \exp(ik\,\boldsymbol{\eta}\cdot\boldsymbol{s})\; d\boldsymbol{s}, \tag{2.2}$$

where $\boldsymbol{r} = (x,y)$ denotes the two-dimensional position vector at a transverse plane, $k\boldsymbol{\eta} = (ku, kv) = (k_x, k_y)$ gives the wavevector components along the Cartesian x and y axes, and $\boldsymbol{s}$ is a vectorial variable. Accordingly, u and v would represent angles of propagation (without taking evanescent waves into account). In Eq. (2.2) the CSD function is expressed in terms of the variables $\boldsymbol{r}$ and $\boldsymbol{s}$, which are related with $\boldsymbol{r}_1$ and $\boldsymbol{r}_2$ by the formulae (see Fig. 2.1):

$$\boldsymbol{r} = \frac{\boldsymbol{r}_1 + \boldsymbol{r}_2}{2}, \tag{2.3a}$$

$$\boldsymbol{s} = \boldsymbol{r}_1 - \boldsymbol{r}_2. \tag{2.3b}$$

The WDF was introduced by Wigner to describe the quantum-mechanics phenomena in the (position-momentum) phase space. Later Walther (1968) demonstrated the role of this function in Optics as a link between partial coherence and

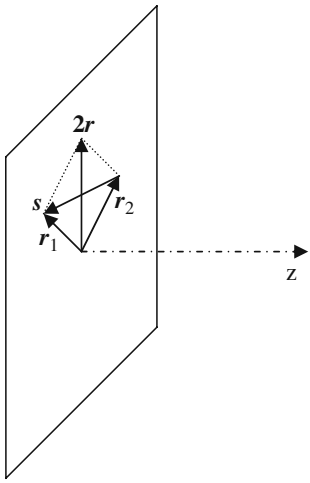

Fig. 2.1 Illustrating the geometrical representation of vectors $\boldsymbol{r}$ and $\boldsymbol{s}$

traditional radiometry: The WDF can physically be understood in Optics as the amplitude associated to a ray passing through a point along a certain direction. Some care, however, should be taken because the WDF could reach negative values in certain cases (Friberg, 1993; Marchand and Wolf, 1974) (unlike the positiveness of the energy content of a ray). Note that integration of $h(\boldsymbol{r},\boldsymbol{\eta},z)$ over the angular variables u and v is proportional to the beam irradiance. Moreover, integration over the spatial variables x and y gives the directional intensity, which is a proportional to the radiant intensity of the field (a factor $\cos^2\alpha$ apart, where α is the angle of observation with respect to the z-axis).

In terms of the WDF, a number of parameters can be defined, which provide an overall spatial description of the field upon propagation. Let us introduce the beam irradiance moments in the form

$$\langle x^m y^n u^p v^q \rangle \equiv \frac{1}{I_o} \iint_{-\infty}^{+\infty} x^m y^n u^p v^q h\,(\boldsymbol{r},\boldsymbol{\eta},z)\, d\boldsymbol{r}\, d\boldsymbol{\eta}, \tag{2.4}$$

where m, n, p, q are integer numbers, the sharp brackets $\langle\ \rangle$ are defined by Eq. (2.4) itself, and

$$I_0 = \iint_{-\infty}^{+\infty} h\,(\boldsymbol{r},\boldsymbol{\eta},z)\, d\boldsymbol{r}\, d\boldsymbol{\eta} \tag{2.5}$$

At each transverse plane, the four first-order beam moments, $\langle x\rangle$, $\langle y\rangle$, $\langle u\rangle$ and $\langle v\rangle$, characterize the center of the beam profile and the mean direction of the field. For simplicity, in what follows it will be assumed that these moments equal zero. This is not a true restriction, since it is equivalent to a shift of the Cartesian coordinate system. In summary, we consider that the z-axis coincides with the mean direction of propagation, and the beam center is placed on this axis at any plane z.

The resulting ten different second-order moments allow a global and meaningful characterization of the spatial structure of a partially coherent quasimonochromatic beam. In terms of them, we may introduce the following parametrization for scalar fields (see, for example, (Giesen and Morin, 1998; Giesen and Weber 2002; Kudryashov et al., 2006; Laabs and Weber, 2000; Mejías et al., 1993; Morin and Giesen, 1996; Weber et al., 1994; WLT, 2001)):

(i) $\langle r^2 \rangle = \langle x^2 + y^2 \rangle$: (Squared) *spatial size* of the beam cross-section, referred to the region where the irradiance takes significant values. In this expression, $\langle x^2 \rangle$ and $\langle y^2 \rangle$ represent (squared) transverse beam widths along the x and y-axes, respectively (see Fig. 2.2). In terms of the beam irradiance, $I(x,y)$, this moment reads

$$\langle x^2 + y^2 \rangle = \frac{\iint_{-\infty}^{+\infty} \left(x^2 + y^2\right) I\,(x,y)\,dxdy}{\iint_{-\infty}^{+\infty} I\,(x,y)\,dxdy}. \tag{2.6}$$

(ii) $\langle \eta^2 \rangle = \langle u^2 + v^2 \rangle$: (Squared) *far-field divergence*, which is connected with the energy distribution associated with each spatial frequency of the beam.

(iii) $\langle \boldsymbol{r} \cdot \boldsymbol{\eta} \rangle = \langle xu + yv \rangle$: This moment provides the position of the *beam waist*, i.e., the plane where the beam width takes its minimum value (see Fig. 2.2). At the

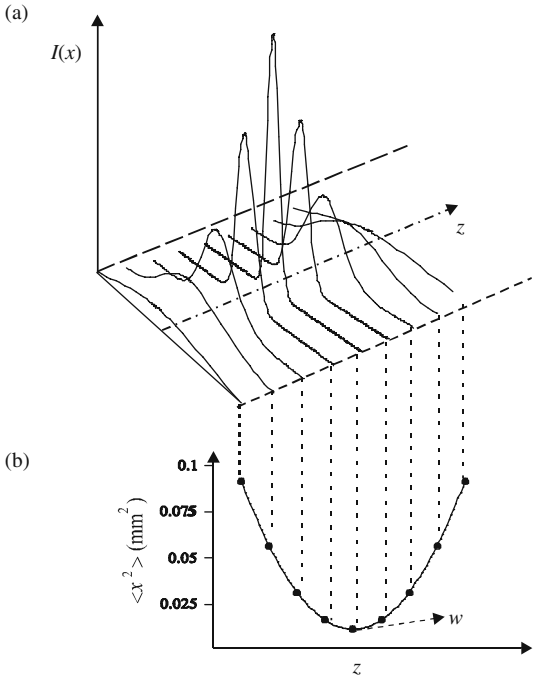

Fig. 2.2 Free propagation of a typical (one-dimensional) Gaussian beam (λ = 633 nm). (**a**) Irradiance profiles at different planes z = constant. (**b**) Parabolic dependence of the second-order moment $\langle x^2 \rangle$ on the propagation distance z. The value w denotes the position of the waist plane (minimum beam width). In the figure, the separation between the successive planes is 125 mm. See also (Mejías et al., 2002)

waist plane, $\langle xu + yv \rangle$ vanishes. It should be remarked that a general astigmatic beam would exhibit different minimum widths, $\langle x^2 \rangle_{\min}$ and $\langle y^2 \rangle_{\min}$ at different positions along z. The global beam waist, whose position z_w is given by the condition

$$\langle xu + yv \rangle = 0, \tag{2.7}$$

refers to the minimum value (under free propagation) of the global second-order moment $\langle r^2 \rangle$. Note, in addition, that $\langle xu \rangle$ and $\langle yv \rangle$ are related to the curvature radii of the beam wavefront by the formulae:

$$R_x = \frac{\langle x^2 \rangle}{\langle xu \rangle}, \tag{2.8}$$

$$R_y = \frac{\langle y^2 \rangle}{\langle yv \rangle}. \tag{2.9}$$

(iv) $\langle xy \rangle$: It gives the orientation (with regard to the laboratory axes) of the so-called *principal axis* of the beam through the condition $\langle xy \rangle = 0$ (Martínez-Herrero and Mejías, 2006a, b; Serna et al., 1991, 1992a, b). It should be noticed that the beam widths $\langle x^2 \rangle^{1/2}$ and $\langle y^2 \rangle^{1/2}$ reach their extreme (maximum and minimum) values along the principal axes (see Fig. 2.3). Since, for general beams, the transverse profile rotates as the field propagates into free space, these axes are used to determine the orientation of the beam profile.

(v) $\langle uv \rangle$: It provides the orientation of the so-called *absolute axes* of the beam (Serna et al., 1991, 1992a, b), defined by the condition $\langle uv \rangle = 0$. Unlike the principal axes, the absolute axes do not rotate upon free propagation, and they constitute an absolute transverse coordinate system with respect to which the orientation of the principal axes can be established.

(vi) $\langle xv \rangle - \langle yu \rangle$: It is related with the *orbital angular momentum* of the global beam (Alieva and Bastiaans, 2004; Allen et al., 2009; Bekshaev et al., 2003; Martínez-Herrero and Mejías, 2006b; Nemes and Siegman, 1994; Vasnetsov et al., 2003). The existence of angular momentum is a consequence of the beam structure and is responsible for the twisting spatial behavior of certain

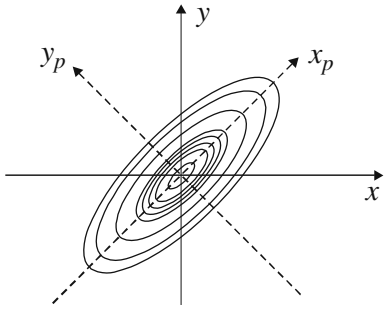

Fig. 2.3 Illustrating the second-order moment <*xy*>. The contour lines of equal irradiance (isophotes) correspond to an astigmatic Gaussian profile at a transverse plane. The principal axes are denoted by x_P,y_P

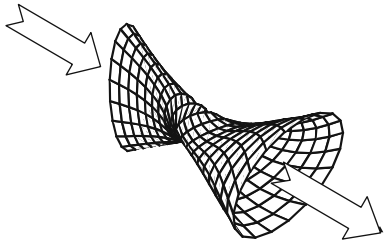

Fig. 2.4 Illustrating the spatial behavior of a twisted Gaussian beam (upon free propagation). The arrows show the propagation direction of the beam. See also (Mejías et al., 2002)

fields under free propagation (see Fig. 2.4). Note, in this sense, that the time-averaged orbital angular-momentum flux, J_z , transported by a beam through a transverse plane z reads

$$J_z = \frac{I_0}{c} \left(\langle xv \rangle - \langle yu \rangle \right). \tag{2.10}$$

where c is the speed of light in vacuum. In particular J_z equals zero for rotationally-symmetric Gaussian fields as well as for Hermite-Gauss beams, but it changes for twisted Gaussian fields (Gori et al., 1994; Nemes and Siegman, 1994; Simon and Mukunda, 1993) or for certain Laguerre-Gauss beams. The reader should realize that, in general, no plane wavefront exists in the waist region, but two cylindrical wavefronts separated by a certain distance. Hence, in a general case, there is no common waist along the orthogonal x- and y-axes.

It is interesting to note that, for deterministic beams represented by a well-defined electric field amplitude E, the above physical parameters can also be directly written in terms of E as follows:

$$\langle r^2 \rangle = \frac{1}{I} \iint r^2 |E(r,\theta)|^2 \, r \, dr \, d\theta, \tag{2.11a}$$

$$\langle \eta^2 \rangle = \frac{1}{k^2 I} \iint \left(\left| \frac{\partial E}{\partial r} \right|^2 + \frac{1}{r^2} \left| \frac{\partial E}{\partial \theta} \right|^2 \right) r \, dr \, d\theta, \tag{2.11b}$$

$$\langle \boldsymbol{r} \cdot \boldsymbol{\eta} \rangle = \frac{1}{k I} \iint r \, \mathrm{Im} \left[E^* \frac{\partial E}{\partial r} \right] r \, dr \, d\theta, \tag{2.11c}$$

$$\langle xy \rangle = \frac{1}{2I} \iint r^2 \, \sin 2\theta \, |E(r,\theta)|^2 \, r \, dr \, d\theta, \tag{2.11d}$$

$$\langle xv - yu \rangle = \frac{1}{k I} \iint \mathrm{Im} \left[E^* \frac{\partial E}{\partial \theta} \right] r \, dr \, d\theta, \tag{2.11e}$$

$$\langle uv \rangle = \frac{1}{k^2 I} \iint \left\{ \frac{\sin 2\theta}{2} \left(\left| \frac{\partial E}{\partial r} \right|^2 - \frac{1}{r^2} \left| \frac{\partial E}{\partial \theta} \right|^2 \right) + \frac{\cos 2\theta}{r} \mathrm{Re} \left[\frac{\partial E^*}{\partial r} \frac{\partial E}{\partial \theta} \right] \right\} r \, dr \, d\theta \tag{2.11f}$$

where $I = \iint |E|^2 r\, dr\, d\theta$ is a normalization factor, proportional to the beam power. For illustrative purposes, in these equations we have used planar polar coordinates r and θ, frequently encountered in the literature. Alternative expressions for the second-order moments can be found, for example, in (Alda et al., 1997; Weber, 1992). Finally, let us briefly remark that the second-order moment $\langle x^2 \rangle$ takes the value $\frac{w^2}{4}$ for a Gaussian amplitude $\exp\left(-\frac{x^2}{w^2}\right)$.

In this section we have focused the attention on the mathematical definition of the irradiance moments. Details for the practical use of the above parameters can be found in the ISO standard 11146.

2.2.2 Propagation and Measurement of the Irradiance Moments

To analytically handle in a compact form the second-order irradiance moments of a scalar beam, they are usually arranged in a 4×4 symmetric matrix, $\hat{M}$, defined, at a certain transverse plane, as follows

$$\hat{M} = \begin{pmatrix} \langle x^2 \rangle & \langle xy \rangle & \langle xu \rangle & \langle xv \rangle \\ \langle xy \rangle & \langle y^2 \rangle & \langle yu \rangle & \langle yv \rangle \\ \langle xu \rangle & \langle yu \rangle & \langle u^2 \rangle & \langle uv \rangle \\ \langle xv \rangle & \langle yv \rangle & \langle uv \rangle & \langle v^2 \rangle \end{pmatrix}. \tag{2.12}$$

We immediately see that all the moments introduced in (i)–(vi) can be written in terms of the elements of matrix $\hat{M}$. The usefulness of this matrix arises from the simple link between the values of $\hat{M}$ at the output and input planes of any first-order optical system. The general propagation law takes the form (Bastiaans, 1989; Serna et al., 1991)

$$\hat{M}_{out} = \hat{P}\, \hat{M}_{inp}\, \hat{P}^t, \tag{2.13}$$

where $\hat{P}$ is the 4×4 ABCD matrix representing the optical system (Siegman, 1986), and the subscripts *out* and *inp* refer to output and input planes, respectively.

It is also important to notice that the second-order moments are measurable quantities. The measurement procedure commonly employs CCD cameras or similar devices such as pyroelectric matrix arrays. Apart from the resolution limit defined by the pixel size of the camera, the main experimental limitation comes from the signal-to-noise ratio of the output signal. Defective pixels, background noise and electronic circuitry, among other noise sources, also reduce the performance of the measurement devices.

The standard method used to determine the second-order moments records the irradiance profile $I(x,y,z)$ at different transverse planes by means of a sensor array camera. From the data supplied by the camera (irradiance versus position), one computes the purely spatial moments $\langle x^2 \rangle$, $\langle y^2 \rangle$ and $\langle xy \rangle$. Since they propagate in free

space according to a parabolic law, by means of a fitting procedure of the experimental data to the parabolic curves we obtain all moments except $\langle xv \rangle$ and $\langle yu \rangle$, which are coupled. They can be determined through a pair of additional measurements by using an auxiliary cylindrical lens. Here we do not proceed further into the experimental procedure. Additional details can be found, for example, in (Mejías et al., 2002).

It should also be mentioned that the above formalism based on the second-order irradiance moments fails in certain cases (e.g., slit diffraction). The main problem arises when one tries to analytically determine the far-field divergence. One finds that this parameter becomes infinite. Any attempt to represent the sharp edge by smooth functions fails too because the second-order moment $\langle \eta^2 \rangle$ takes higher values as the fit improves, and, in the limit, tends to infinite again. Although, on the basis of the moments formalism, second-order characteristic beam parameters were generalized for fields crossing through hard-edge openings (Martínez-Herrero and Mejías, 1993b, Martínez-Herrero et al., 1995c; Martínez-Herrero et al., 2003b), this is a problem whose analytical solution deserves further study in the future.

Let us finally remark that generalization of the above scalar formalism to light pulses (nanoseconds) can be found in (Mejías and Martínez-Herrero, 1995; Encinas-Sanz et al., 1998).

2.3 Second-Order Overall Characterization: Vectorial Case

In Chap. 1 we pointed out that partially polarized beams and polarization-altering optical devices could be mathematically modelled by using the Stokes vectors and Müller matrices. It was implicitly assumed, however, a uniform polarization distribution across the beam profile. In the present section we will generalize the Stokes formalism in order to characterize the overall spatial structure of a polarized light field. The propagation laws through optical systems will also be investigated. This formalism extends the description based on the irradiance moments, reported in the previous section for the scalar case, to non-uniformly polarized beams.

2.3.1 The Wigner Matrix

Let us again consider an electromagnetic field propagating essentially along the z axis. Assuming that the longitudinal component of the field is negligible, the electric field vector reads (within the paraxial approach)

$$\boldsymbol{E}\left(\boldsymbol{r},z\right) = \left(E_s\left(\boldsymbol{r},z\right), E_p\left(\boldsymbol{r},z\right)\right). \tag{2.14}$$

For the sake of convenience, the position vector $\boldsymbol{r} = (x,y)$ is defined in the present section as the product of the wavenumber k by the transverse Cartesian coordinates of the point at which the field is determined. To avoid any confusion, we will write the dimensionless position vector $k\boldsymbol{r}$ in the form $\tilde{\boldsymbol{r}} \equiv k\boldsymbol{r}$.

For vectorial beamlike fields, it is customary to employ their cross-spectral density matrix (Born and Wolf, 1999; Mandel and Wolf, 1995; Perina, 1971; Wolf, 2007), namely,

$$\hat{W}(\tilde{\boldsymbol{r}}_1,\tilde{\boldsymbol{r}}_2) = \overline{\boldsymbol{E}^{\dagger}(\tilde{\boldsymbol{r}}_1,z)\,\boldsymbol{E}(\tilde{\boldsymbol{r}}_2,z)}, \tag{2.15}$$

where

$$\boldsymbol{E}^{\dagger} = \begin{pmatrix} E_s^* \\ E_p^* \end{pmatrix}. \tag{2.16}$$

In terms of $\hat{W}$, we can now introduce the so-called Wigner matrix, $\hat{H}$, defined in the form (Martínez-Herrero and Mejías, 1997b)

$$\hat{H}(\tilde{\boldsymbol{r}},\boldsymbol{\eta},z) = \frac{1}{k^2}\iint \hat{W}\left(\tilde{\boldsymbol{r}}+\frac{\boldsymbol{s}}{2},\tilde{\boldsymbol{r}}-\frac{\boldsymbol{s}}{2}\right)\exp(i\boldsymbol{\eta}\cdot\boldsymbol{s})d\boldsymbol{s}, \tag{2.17}$$

where $\tilde{\boldsymbol{r}} = (\tilde{\boldsymbol{r}}_1+\tilde{\boldsymbol{r}}_2)/2$ and $\boldsymbol{s} = \tilde{\boldsymbol{r}}_1-\tilde{\boldsymbol{r}}_2$ as in the previous section. No confusion should arise from the fact that the symbol H is also commonly used for the magnetic field, because the Wigner matrix always appears with a caret.

Matrix $\hat{H}$ can also be written in the form

$$\hat{H}(\tilde{\boldsymbol{r}},\boldsymbol{\eta},z) = \begin{pmatrix} h_{ss}(\tilde{\boldsymbol{r}},\boldsymbol{\eta},z) & h_{sp}(\tilde{\boldsymbol{r}},\boldsymbol{\eta},z) \\ h_{ps}(\tilde{\boldsymbol{r}},\boldsymbol{\eta},z) & h_{pp}(\tilde{\boldsymbol{r}},\boldsymbol{\eta},z) \end{pmatrix}, \tag{2.18}$$

where

$$h_{ij}(\tilde{\boldsymbol{r}},\boldsymbol{\eta},z) = \frac{1}{k^2}\iint \overline{E_i^*\left(\tilde{\boldsymbol{r}}+\frac{\boldsymbol{s}}{2},z\right)E_j\left(\tilde{\boldsymbol{r}}-\frac{\boldsymbol{s}}{2},z\right)}\exp(i\boldsymbol{s}\cdot\boldsymbol{\eta})d\boldsymbol{s}; \quad i,j = s,p. \tag{2.19}$$

It should be noted that the diagonal elements of $\hat{H}$ represent the WDF associated to each transverse component of the whole beam. In addition, the off-diagonal elements h_{sp} and h_{ps} accounts for the correlation between the two transverse components of the field. In the scalar framework, only the diagonal elements of the Wigner matrix would be considered.

2.3.2 The Stokes Matrices

Let us now define the so-called Stokes matrices in the form (Martínez-Herrero et al., 1997b)

$$\hat{S}_n = \iint \boldsymbol{R}^t\boldsymbol{R}\,\mathrm{Tr}\left(\hat{\sigma}_n\hat{H}(\tilde{\boldsymbol{r}},\boldsymbol{\eta})\right)d\tilde{\boldsymbol{r}}d\boldsymbol{\eta}, \quad n = 0,1,2,3, \tag{2.20}$$

where

$$\boldsymbol{R} = (\tilde{\boldsymbol{r}},\boldsymbol{\eta}) = (x,y,u,v) \tag{2.21}$$

is a 1×4 vector, $\hat{\sigma}_0$ denotes here the 2×2 identity matrix and $\hat{\sigma}_1$,$\hat{\sigma}_2$ y $\hat{\sigma}_3$ are again the Pauli matrices. For the sake of convenience, we introduce the following notation

$$[\alpha\beta]_{ij} = \iint \alpha\beta h_{ij}(\tilde{\boldsymbol{r}},\boldsymbol{\eta},z)d\tilde{\boldsymbol{r}}d\boldsymbol{\eta}; \qquad i,j = s,p;\ \alpha,\beta = x,\ y,\ u,\ v, \tag{2.22}$$

along with

$$[\alpha\beta]_0 \equiv [\alpha\beta]_{ss} + [\alpha\beta]_{pp}\,, \tag{2.23a}$$

$$[\alpha\beta]_1 \equiv [\alpha\beta]_{ss} - [\alpha\beta]_{pp} \tag{2.23b}$$

$$[\alpha\beta]_2 \equiv [\alpha\beta]_{sp} + [\alpha\beta]_{ps}\,, \tag{2.23c}$$

$$[\alpha\beta]_3 \equiv i\left([\alpha\beta]_{sp} - [\alpha\beta]_{ps}\right), \tag{2.23d}$$

where the subscripts 0, 1, 2 and 3 refer to the corresponding Stokes matrices.

As is quite apparent from Eq. (2.22), $[\alpha\beta]_{ij}$ are closely related with the second-order moments of the WDF defined for scalar fields (cf. Eq. (2.4)). Moreover, the quantities $[\alpha\beta]_n$, $n = 0, 1, 2, 3$, resembles the structure of the conventional Stokes parameters. It should also be noted that the present treatment reduces to the scalar one for the particular case of uniformly linearly-polarized beams. In particular, the standard Stokes parameters can be considered themselves as zero-order irradiance moments.

Let us now write matrix $\hat{S}_0$ as follows

$$\hat{S}_0 = \begin{pmatrix} \hat{\mathrm{W}}_0^2 & \hat{\boldsymbol{\Psi}}_0 \\ \hat{\boldsymbol{\Psi}}_0^{\,t} & \hat{\boldsymbol{\Phi}}_0^{\,2} \end{pmatrix}, \tag{2.24}$$

where

$$\hat{\mathrm{W}}_0^2 \equiv \begin{pmatrix} [x^2]_0 & [xy]_0 \\ [xy]_0 & [y^2]_0 \end{pmatrix}, \tag{2.25a}$$

$$\hat{\boldsymbol{\Phi}}_0^{\,2} \equiv \begin{pmatrix} [u^2]_0 & [uv]_0 \\ [uv]_0 & [v^2]_0 \end{pmatrix}, \tag{2.25b}$$

$$\hat{\boldsymbol{\Psi}}_0 \equiv \begin{pmatrix} [xu]_0 & [xv]_0 \\ [yu]_0 & [yv]_0 \end{pmatrix}. \tag{2.25c}$$

These 2×2 matrices contain the overall spatial characteristics of the beam, namely,

– the spatial structure of the transverse irradiance profile in the near field (matrix $\hat{\mathrm{W}}_0^2$).
– the divergence of the beam (beam spread) at the far field (matrix $\hat{\boldsymbol{\Phi}}_0^2$).
– the orbital angular moment of the beam (matrix $\hat{\boldsymbol{\Psi}}_0$).
– the averaged curvature radius (elements $[xu]_0$, $\left[yv\right]_0$).

In other words, matrix $\hat{S}_0$ gives, in the vectorial case, a similar information to that provided by the beam matrix, $\hat{M}$, in the scalar case. As a matter of fact, the elements of both matrices are related through the formulae

$$\langle x^2\rangle = \frac{\left[x^2\right]_0}{4\pi^2 k^2 I}; \quad \langle y^2\rangle = \frac{\left[y^2\right]_0}{4\pi^2 k^2 I}, \tag{2.26a}$$

$$\langle u^2\rangle = \frac{\left[u^2\right]_0}{4\pi^2 I}; \quad \langle v^2\rangle = \frac{\left[v^2\right]_0}{4\pi^2 I}, \tag{2.26b}$$

$$\langle xu\rangle = \frac{[xu]_0}{4\pi^2 kI}; \quad \langle yv\rangle = \frac{\left[yv\right]_0}{4\pi^2 kI}, \tag{2.26c}$$

$$\langle xv\rangle = \frac{[xv]_0}{4\pi^2 kI}; \quad \langle yu\rangle = \frac{\left[yu\right]_0}{4\pi^2 kI}, \tag{2.26d}$$

$$\langle xy\rangle = \frac{\left[xy\right]_0}{4\pi^2 k^2 I}; \quad \langle uv\rangle = \frac{[uv]_0}{4\pi^2 I}, \tag{2.26e}$$

where

$$I = \frac{1}{4\pi^2}\iint \mathrm{Tr}\,\hat{H}\, d\tilde{\boldsymbol{r}}\, d\boldsymbol{\eta}, \tag{2.27}$$

and $<\alpha\beta>$, $\alpha, \beta = x, y, u, v$, are the second-order irradiance moments defined for scalar fields in the previous section. It is important to note that, on the contrary to that occurs concerning the dimensionless squared brackets, the spatial variables inside the sharp brackets keep their usual dimensions (for example, $<xu>$ exhibits dimension of length).

Equations (2.26) allow to conclude that the spatial parameters introduced in the scalar case can be obtained from the knowledge of the elements of the Stokes matrix $\hat{S}_0$.

Let us finally remark the formal analogy between the well-known inequality satisfied by the standard Stokes parameters,

$$s_0^2 \geq s_1^2 + s_2^2 + s_3^2, \tag{2.28}$$

and the diagonal elements of the Stokes matrices:

$$\left(\mathrm{Tr}\,\hat{S}_0\right)^2 \geq \left(\mathrm{Tr}\,\hat{S}_1\right)^2 + \left(\mathrm{Tr}\,\hat{S}_2\right)^2 + \left(\mathrm{Tr}\,\hat{S}_3\right)^2. \tag{2.29}$$

On the basis of this condition, a rather rough but simple classification scheme of partially polarized beams can be outlined.

Any beam should belong to one of the following three categories:

(a) *Second-order totally polarized beams*.
These are beams fulfilling

$$\left(\mathrm{Tr}\,\hat{S}_0\right)^2 = \left(\mathrm{Tr}\,\hat{S}_1\right)^2 + \left(\mathrm{Tr}\,\hat{S}_2\right)^2 + \left(\mathrm{Tr}\,\hat{S}_3\right)^2. \tag{2.30}$$

Belong to this type of fields, those uniformly totally polarized (UTP) beams whose Cartesian components of the electric field vector are proportional, i.e.,

$$E_s(\boldsymbol{r}) = \alpha E_p(\boldsymbol{r}), \tag{2.31}$$

where α is a complex number.

(b) *Second-order non-polarized beams*.
These are beams fulfilling

$$\mathrm{Tr}\,\hat{S}_1 = \mathrm{Tr}\,\hat{S}_2 = \mathrm{Tr}\,\hat{S}_3 = 0. \tag{2.32}$$

Belong to this category those locally unpolarized beams (i.e., $P(\boldsymbol{r}) = 0$ everywhere) whose divergences along de s- and p- directions take the same value ($[\eta^2]_{ss} = [\eta^2]_{pp}$). Of course, this is not the only example. We could also mention, for instance, radial or azimuthally totally-polarized beams (see Chap. 1 and references therein).

(c) *Second-order partially polarized beams*.
These fields are defined through the inequality

$$\left(\mathrm{Tr}\,\hat{S}_0\right)^2 > \left(\mathrm{Tr}\,\hat{S}_1\right)^2 + \left(\mathrm{Tr}\,\hat{S}_2\right)^2 + \left(\mathrm{Tr}\hat{S}_3\right)^2. \tag{2.33}$$

Beams not included in the categories (a) and (b) belong to this type.

2.3.3 Propagation Laws and Measurement

Let us now report the propagation laws of the Stokes matrices through optical systems. Attention will be focused on three kind of devices.

i. *First-order optical (ABCD) systems*
It can be shown that the general propagation law for the Stokes matrices, propagating through first-order systems represented by 4×4 matrices $\hat{P} = \begin{pmatrix} \hat{A} & \hat{B} \\ \hat{C} & \hat{D} \end{pmatrix}$, reads

$$\hat{S}_n^{out} = \hat{P}'\hat{S}_n^{inp}(\hat{P}')^t \qquad n = 0,1,2,3\ , \tag{2.34}$$

which is formally identical to Eq. (2.13) for the scalar case. In this equation, the superscripts *out* and *inp* refer to the output and input planes of the ABCD system, and

$$\hat{P}' \equiv \begin{pmatrix} \hat{A}' & \hat{B}' \\ \hat{C}' & \hat{D}' \end{pmatrix} \tag{2.35}$$

where $\hat{A}' = \hat{A}$, $\hat{B}' = k\hat{B}$, $\hat{C}' = \frac{1}{k}\hat{C}$ and $\hat{D}' = \hat{D}$. The changes should be introduced because, in the Wigner-Stokes formalism, we are using dimensionless position variables. Thus, although $\hat{A}$ and $\hat{D}$ are dimensionless, the elements of matrix $\hat{B}$ are expressed in units of length and the elements of $\hat{C}$ are given in units of the inverse of length.

Two immediate consequences can be obtained from the propagation law (2.34):

(a) The Stokes matrices propagate through ABCD optical systems independently each other.
(b) There are two kinds of beams that retain the same character (with regard to the polarization) after propagation through ABCD systems:

– Uniformly totally polarized beams.
– Second-order non-polarized beams for which (Martínez-Herrero et al., 1997b; Mejías et al., 2002)

$$\hat{S}_1 = \hat{S}_2 = \hat{S}_3 = 0. \tag{2.36}$$

ii. *Spatially-uniform polarization-altering (SUPA) systems*
They are optical devices whose components modify the polarization state of the light in a uniform way throughout the beam cross-section. They are described by Müller matrices with constant elements.

In this case, the general propagation law for the Stokes matrices becomes (Martínez-Herrero et al., 1997b)

$$\hat{S}_n^{out} = \sum_{m=0}^{3} \hat{\mathcal{M}}_{nm} \hat{S}_m^{inp}, \quad n,m = 0,1,2,3, \tag{2.37}$$

where $\hat{\mathcal{M}}_{nm}$ denote the elements of the Müller matrix. It is important to notice that, unlike to that occurs for first-order optical systems, the Stokes matrices, in general, do not propagate through SUPA systems independently each other: Each Stokes matrix at the output of such kind of systems depends, in principle, on the values of the four Stokes matrices associated to the incident beam.

iii. *Mixed systems*
They should be understood as the combination of first-order optical systems and SUPA devices cascaded in an arbitrary way. This kind of systems exhibits two analytical properties:

(a) The ABCD matrix that represents a first-order optical component commutes with the Müller matrix associated to a SUPA device. Note, however,

that two ABCD matrices, in general, does not commute. The same applies for the Müller matrices.

(b) All the ABCD components of a mixed system, represented by the dimensionless matrices $\hat{P}_n$, $n = 1,2\ldots,N$, can be reduced to an equivalent first-order optical device whose ABCD matrix, $\hat{P}^{eq}$, is given by

$$\hat{P}^{eq} = \prod_{n=0}^{N} \hat{P}_n \tag{2.38}$$

In asimilar way, all the SUPA devices of a mixed system, represented by the Müller matrices $\hat{\mathcal{M}}_m$, $m = 1, 2\ldots, M$, can be reduced to an equivalent SUPA component whose Müller matrix $\hat{\mathcal{M}}^{eq}$ is

$$\hat{\mathcal{M}}^{eq} = \prod_{m=0}^{M} \hat{\mathcal{M}}_m. \tag{2.39}$$

Taking the above properties into account, it can be shown that the propagation law of the Stokes matrices of a general beam through mixed systems reads

$$\hat{S}_p^{out} = \hat{P}^{eq} \left(\sum_{q=0}^{3} \hat{\mathcal{M}}_{pq}^{eq} \hat{S}_q^{inp} \right) \left(\hat{P}^{eq} \right)^t, \; p,q = 0,1,2,3, \tag{2.40}$$

or, making use of the commutative property,

$$\hat{S}_p^{out} = \sum_{q=0}^{3} \hat{\mathcal{M}}_{pq}^{eq} \left(\hat{P}^{eq} \hat{S}_q^{inp} \right) \left(\hat{P}^{eq} \right)^t, \; p,q = 0,1,2,3. \tag{2.41}$$

Let us finally remark that all the elements of the four Stokes matrices are measurable quantities. The procedure to determine the Stokes matrices is based on the well-known procedure to get the conventional Stokes parameters. Accordingly, a mixed system composed of a quarter-wave plate, a free propagation distance and a linear polarizer is used. The key of the method is to link matrix

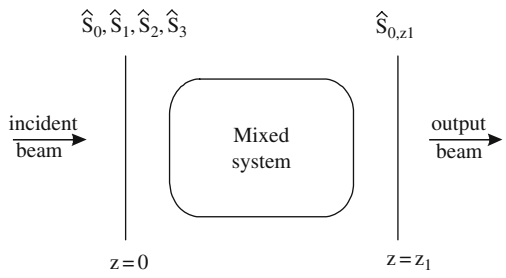

Fig. 2.5 Illustrating the basis of the procedure employed to determine the Stokes matrices

$\hat{S}_0$ at a plane $z = z_1$ with the Stokes matrices at the plane $z = 0$ where we want to measure their values (see Fig. 2.5).
Since the elements of $\hat{S}_0$ are connected with the second-order irradiance moments, our measurement problem reduces to obtain such moments. Here we do not proceed further into the details of the experimental methods used to find the Stokes matrices (see, in this connection, (Mejías et al., 2002) and references therein).

2.3.4 Invariant Parameters

In terms of the Wigner-Stokes formalism, we are now going to introduce certain overall parameters that remain invariant upon propagation through rotationally-symmetric first-order optical systems. In addition, these parameters do not change under rotation of the transverse Cartesian axes with respect to which the electric field components are given.

To begin with, let us first define a matrix $\hat{T}$ in the form

$$\hat{T} = \begin{pmatrix} \tilde{\boldsymbol{r}} \cdot \tilde{\boldsymbol{r}} & \tilde{\boldsymbol{r}} \cdot \boldsymbol{\eta} \\ \boldsymbol{\eta} \cdot \tilde{\boldsymbol{r}} & \boldsymbol{\eta} \cdot \boldsymbol{\eta} \end{pmatrix}, \tag{2.42}$$

where $\tilde{\boldsymbol{r}}$ is again the dimensionless position vector. In terms of the elements of matrix $\hat{T}$, the following 2×2 matrices can be introduced (Martínez-Herrero and Mejías, 2007):

$$\hat{\zeta}_n = \int \hat{T}\ \mathrm{Tr}\left(\hat{\sigma}_n \hat{H}\right) d\tilde{\boldsymbol{r}} d\boldsymbol{\eta},\ n = 0,1,2,3, \tag{2.43}$$

which are expressed in explicit form as follows:

$$\hat{\zeta}_0 = \begin{pmatrix} \left[\tilde{r}^2\right]_{ss} + \left[\tilde{r}^2\right]_{pp} & \left[\tilde{\boldsymbol{r}} \cdot \boldsymbol{\eta}\right]_{ss} + \left[\tilde{\boldsymbol{r}} \cdot \boldsymbol{\eta}\right]_{pp} \\ \left[\tilde{\boldsymbol{r}} \cdot \boldsymbol{\eta}\right]_{ss} + \left[\tilde{\boldsymbol{r}} \cdot \boldsymbol{\eta}\right]_{pp} & \left[\eta^2\right]_{ss} + \left[\eta^2\right]_{pp} \end{pmatrix}, \tag{2.44a}$$

$$\hat{\zeta}_1 = \begin{pmatrix} \left[\tilde{r}^2\right]_{ss} - \left[\tilde{r}^2\right]_{pp} & \left[\tilde{\boldsymbol{r}} \cdot \boldsymbol{\eta}\right]_{ss} - \left[\tilde{\boldsymbol{r}} \cdot \boldsymbol{\eta}\right]_{pp} \\ \left[\tilde{\boldsymbol{r}} \cdot \boldsymbol{\eta}\right]_{ss} - \left[\tilde{\boldsymbol{r}} \cdot \boldsymbol{\eta}\right]_{pp} & \left[\eta^2\right]_{ss} - \left[\eta^2\right]_{pp} \end{pmatrix}, \tag{2.44b}$$

$$\hat{\zeta}_2 = 2\mathrm{Re}\begin{pmatrix} \left[\tilde{r}^2\right]_{sp} & \left[\tilde{\boldsymbol{r}} \cdot \boldsymbol{\eta}\right]_{sp} \\ \left[\tilde{\boldsymbol{r}} \cdot \boldsymbol{\eta}\right]_{sp} & \left[\eta^2\right]_{sp} \end{pmatrix}, \tag{2.44c}$$

$$\hat{\zeta}_3 = 2\mathrm{Im}\begin{pmatrix} \left[\tilde{r}^2\right]_{sp} & \left[\tilde{\boldsymbol{r}} \cdot \boldsymbol{\eta}\right]_{sp} \\ \left[\tilde{\boldsymbol{r}} \cdot \boldsymbol{\eta}\right]_{sp} & \left[\eta^2\right]_{sp} \end{pmatrix}. \tag{2.44d}$$

It can be shown that $\hat{\zeta}_n$, $n = 0,1,2,3$, also read

$$\hat{\zeta}_n = \begin{pmatrix} \mathrm{Tr}\,(S_{11})_n & \mathrm{Tr}\,(S_{12})_n \\ \mathrm{Tr}\,(S_{21})_n & \mathrm{Tr}\,(S_{22})_n \end{pmatrix}, \tag{2.45}$$

where $(S_{11})_n$, $(S_{12})_n$, $(S_{21})_n$ and $(S_{22})_n$ denote the 2×2 matrices associated to the 4×4 Stokes matrix $\hat{S}_n$, namely

$$\hat{S}_n = \begin{pmatrix} (S_{11})_n & (S_{12})_n \\ (S_{21})_n & (S_{22})_n \end{pmatrix}. \tag{2.46}$$

For example,

$$(S_{11})_0 \equiv \hat{W}_0^2 \equiv \begin{pmatrix} [x^2]_0 & [xy]_0 \\ [xy]_0 & [y^2]_0 \end{pmatrix} \equiv \begin{pmatrix} [x^2]_{ss} + [x^2]_{pp} & [xy]_{ss} + [xy]_{pp} \\ [xy]_{ss} + [xy]_{pp} & [y^2]_{ss} + [y^2]_{pp} \end{pmatrix}, \tag{2.47a}$$

$$(S_{12})_0 \equiv (S_{21})_0^t \equiv \hat{\Psi}_0 \equiv \begin{pmatrix} [xu]_0 & [xv]_0 \\ [yu]_0 & [yv]_0 \end{pmatrix} \equiv \begin{pmatrix} [xu]_{ss} + [xu]_{pp} & [xv]_{ss} + [xv]_{pp} \\ [yu]_{ss} + [yu]_{pp} & [yv]_{ss} + [yv]_{pp} \end{pmatrix}, \tag{2.47b}$$

$$(S_{22})_0 \equiv \hat{\Phi}_0^2 \equiv \begin{pmatrix} [u^2]_0 & [uv]_0 \\ [uv]_0 & [v^2]_0 \end{pmatrix} \equiv \begin{pmatrix} [u^2]_{ss} + [u^2]_{pp} & [uv]_{ss} + [uv]_{pp} \\ [uv]_{ss} + [uv]_{pp} & [v^2]_{ss} + [v^2]_{pp} \end{pmatrix}, \tag{2.47c}$$

and so on.

Recall that the Stokes matrices $\hat{S}_n$ provide an overall description of non-uniformly partially-polarized beams through general optical systems (including polarization-altering devices). In a complementary way, the matrices $\hat{\zeta}_n$ can be of use to characterize such beams through rotationally-symmetric ABCD systems.

To further clarify this point, let us first report several properties of these polarization matrices:

(i) $\mathrm{Tr}\,\hat{\zeta}_n = \mathrm{Tr}\,\hat{S}_n$. This follows at once from Eqs. (2.45) and (2.46).

(ii) For matrices $\hat{\zeta}_n$, the propagation law through rotationally-symmetric first-order optical systems takes the form

$$\left(\hat{\zeta}_n\right)_{output} = \hat{P}' \left(\hat{\zeta}_n\right)_{input} (\hat{P}')^t \; n = 0,1,2,3, \tag{2.48}$$

where the 2×2 dimensionless matrix $\hat{P}'$ was defined in Eq. (2.35). Note that Eq.(2.48) is formally identical to the propagation law of the Stokes matrices through ABCD systems.

(iii) Under rotation of the transverse Cartesian axes around the propagation direction z, the matrices $\hat{\zeta}_n$ become

$$\hat{\zeta}_0' = \hat{\zeta}_0; \tag{2.49a}$$

$$\hat{\zeta}_3' = \hat{\zeta}_3, \tag{2.49b}$$

$$\hat{\zeta}_1' = \cos 2\theta \; \hat{\zeta}_1 + \sin 2\theta \; \hat{\zeta}_2, \tag{2.49c}$$

$$\hat{\zeta}_2' = -\sin 2\theta \; \hat{\zeta}_1 + \cos 2\theta \; \hat{\zeta}_2, \tag{2.49d}$$

where the primes denote the matrices after rotation, and θ is the rotation angle. To get this result we have taken into account that the electric field components read after rotation

$$E_s' = \cos\,\theta\, E_s + \sin\theta\, E_p \tag{2.50a}$$

$$E_p' = -\sin\theta\, E_s + \cos\theta\, E_p \tag{2.50b}$$

In terms of matrices $\hat{\zeta}_n$, a number of invariant overall parameters can be introduced:

(i) $\mathrm{Det}\hat{\zeta}_0$ (2.51)

(ii) $\mathrm{Det}\hat{\zeta}_3$ (2.52)

(iii) $\mathrm{Det}\hat{\zeta}_1 + \mathrm{Det}\hat{\zeta}_2$. (2.53)

It follows from the propagation law (2.48) that these three parameters remain constant when the beam propagates along rotationally-symmetric optical systems (which are the most frequently encountered in the literature). Accordingly, these invariant parameters can be used as suitable labels to characterize, in an analytical way, the spatial distribution of the polarization state of beams propagating through this type of systems. Moreover, since the elements of the Stokes matrices are measurable quantities, the same applies for these parameters. Note that they are also invariant upon rotation of the transverse Cartesian axes.

Let us finally point out that a family of additional invariants can easily be derived from the former ones. Here we only mention two of them:

(a) $$\mathfrak{M} = \mathrm{Det}\hat{\zeta}_0 - \sum_{i=1}^{3} \mathrm{Det}\hat{\zeta}_i, \tag{2.54}$$

(b) and

$$\mathfrak{N} = \frac{2\mathrm{Det}\hat{\zeta}_0 \left| \sum_{i=1}^{3} \mathrm{Det}\hat{\zeta}_i \right|}{\left(\mathrm{Det}\hat{\zeta}_0 + \left| \sum_{i=1}^{3} \mathrm{Det}\hat{\zeta}_i \right| \right)^2}, \tag{2.55}$$

with $0 \leq \mathfrak{N} \leq 1$.

As is clear from the invariance properties of parameters (2.51), (2.52), and (2.53), $\mathfrak{M}$ and $\mathfrak{N}$ inherit this behaviour, namely, $\mathfrak{M}$ and $\mathfrak{N}$ do not change upon both, propagation through rotationally-symmetric ABCD systems and rotation of the transverse coordinate axes. We do not proceed further into the applications of the invariant parameters. This point deserves more study in the future.

2.4 Generalized Degree of Polarization

As we pointed out earlier (see Chap. 1), when we deal with non-uniformly polarized beams, the point-dependent information about the polarization state is provided by the local degree of polarization, $P(\boldsymbol{r})$, defined in Sect. 1.2. However, $P(\boldsymbol{r})$ is not a parameter or figure of merit, but a function.

In the following, a global parameter will be considered in order to characterize both the polarization state and its uniformity across the transverse profile of a general partially polarized beam.

2.4.1 Definition and Properties of Generalized Degree of Polarization

Within the framework of the Wigner-Stokes formalism, let us introduce the so-called generalized degree of polarization, defined at a transverse plane in the form (Movilla et al., 1998)

$$P_G = \sqrt{\frac{\left(\mathrm{Tr}\ \hat{S}_1\right)^2 + \left(\mathrm{Tr}\ \hat{S}_2\right)^2 + \left(\mathrm{Tr}\ \hat{S}_3\right)^2}{\left(\mathrm{Tr}\ \hat{S}_0\right)^2}} = \sqrt{\frac{\left(\mathrm{Tr}\ \hat{\boldsymbol{\xi}}_1\right)^2 + \left(\mathrm{Tr}\ \hat{\boldsymbol{\xi}}_2\right)^2 + \left(\mathrm{Tr}\ \hat{\boldsymbol{\xi}}_3\right)^2}{\left(\mathrm{Tr}\ \hat{\boldsymbol{\xi}}_0\right)^2}}. \tag{2.56}$$

Note that the second equality follows from the property (i) of matrices $\hat{\boldsymbol{\xi}}_n$, n = 0,1,2,3 (see Sect. 2.3).

As is quite evident from this definition, P_{G} exhibits a similar analytical structure to the standard degree of polarization P. Furthermore, this formal similarity extends to two main properties, namely,

(i) $$0 \leq P_G \leq 1, \tag{2.57}$$

and

(ii) P_{G} is independent of the choice of the Cartesian s- and p-axis. Note, in this sense, that P_{G} is given in terms of the traces of symmetric matrices, which are rotationally invariant (around the z-axis).

It can also be shown that $P_G = 1$ for second-order totally polarized beams, and $P_G = 0$ for second-order non-polarized beams. Moreover, it follows at once that P_{G} remains invariant under propagation through ABCD systems for two kind of fields, namely, uniformly totally polarized beams, and second-order non-polarized beams fulfilling $\hat{S}_1 = \hat{S}_2 = \hat{S}_3 = 0$.

A final property concerns the propagation of P_{G}: this parameter satisfies the same law that governs to the Stokes matrices, restricted to their diagonal elements.

2.4.2 Physical Meaning and Measurement

For non-uniformly totally polarized beams, the generalized degree of polarization provides a measure of the uniformity of the polarization over the regions of the beam profile where the irradiance is not negligible. This can be illustrated by means of the following example.

Let us consider a non-uniformly totally-polarized beam whose electric field vector $\boldsymbol{E}$ at the plane $z = 0$ is given by the Jones vector (Movilla et al., 1998)

$$\mathbf{E}(r) = \begin{pmatrix} E_s(r) \\ E_p(r) \end{pmatrix} = E_o \exp\left[-\left(\frac{r}{w_0} \right)^2 \right] \begin{pmatrix} \cos\left[f(r) \right] \\ \sin\left[f(r) \right] \end{pmatrix}, \tag{2.58}$$

with

$$f(r) = \frac{\pi}{2} \exp\left[-(ar)^n \right], \; n = 16, \tag{2.59}$$

where E_0 is a constant amplitude factor, r denotes the radial polar coordinate, w_0 represents the beam size at the waist plane and a^{-1} is a measure of the width of the superGaussian function $f(r)$. Thus, the beam given by Eq. (2.58) exhibits a Gaussian irradiance profile and, at each point of its cross-section, the field is linearly polarized whose azimuth depends on the distance to the propagation axis z.

The spatially-distributed polarization of this beam is illustrated in Fig. 2.6a and c for three different values of the dimensionless product aw_0: Inside the circle whose radius is $\approx a^{-1}$ the beam closely behaves as a uniformly linearly polarized field with negligible s-component. Outside such a circle, the field remains uniformly polarized but now with $E_p \approx 0$. The abrupt transition between both regions is a direct consequence of the high superGaussian character ($n = 16$) of function $f(r)$.

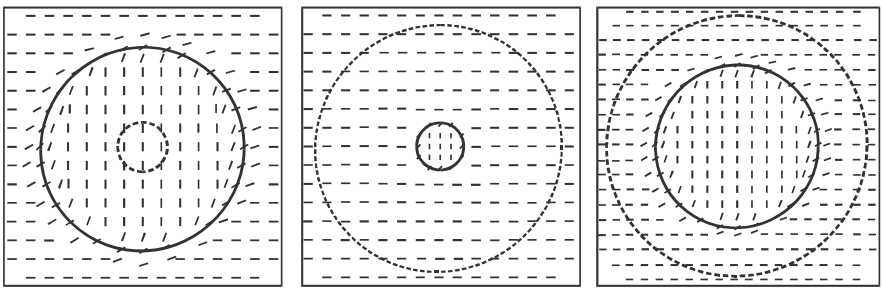

Fig. 2.6 Spatial distribution of the polarization state of the field $\boldsymbol{E}$ given by Eq. (2.58) at the transverse plane $z = 0$. The radii of the circles are $1/a$ (continuous line) and w_0 (dashed line). The small segments show the local orientation of the linearly polarized field. See also (Movilla et al., 1998)

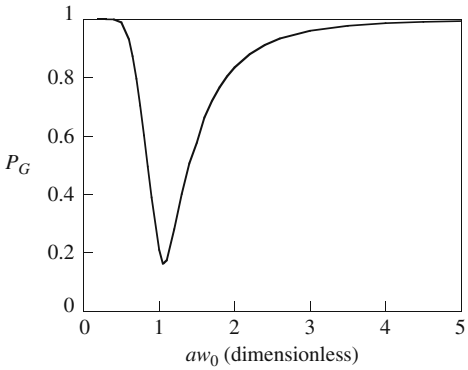

Fig. 2.7 Generalized degree of polarization P_G versus the dimensionless product aw_0. See also (Movilla et al., 1998)

In Fig. 2.6a (with aw_0<<1) the beam is nearly *p*-polarized inside the solid-line circle, which is the region where the irradiance takes significant values. On the other hand, in Fig. 2.6b (with aw_0>>1) the beam behaves as *s*-polarized over the whole transverse profile except over a small region around its center. Finally, in Fig. 2.6c (with $aw_0 \approx 1$) the overall irradiance associated to the *s*- and *p*-regions are balanced.

It is illustrative to calculate the generalized degree of polarization in terms of the product aw_0. This is represented in Fig. 2.7.

Parameter P_G approaches unity for the cases shown in Fig. 2.5a and b, butP_G drastically reduces ($P_G < 0.3$) when aw_0 approaches 1 (Fig. 2.5c).

In summary, we conclude for the example presented here (totally polarized field) that values of P_G nearly 1 means that the beam essentially behaves as uniformly polarized, at least across the region of the beam profile where the irradiance is significant. The opposite case, $P_G \approx 0$, would imply the lack of a global definite polarization over such peak irradiance.

The parameter P_G can be experimentally determined from the measurement of the traces of the Stokes matrices. In the following we briefly describe two procedures to determine them. Both methods involve the measurement of the total power together with the beam width and divergence for several orientations of a polarizer and a quarter-wave plate at an observation plane, which remains unchanged during the procedure.

Method A

It follows four steps (Movilla et al., 2000):

Step 1

Measurement of the global power, I, (squared) beam width $\langle r^2 \rangle$, and (squared) far-field divergence $\langle \eta^2 \rangle$ at the observation plane after free propagation. Here, the measurements are performed with no use of any polarizing element.

Step 2

Measurement of the same parameters as before but now the beam travels through a polarizer which accepts linear polarization in the azimuth $\alpha = 0°$, where α indicates the orientation of the transmission axis of the polarizer with respect to the *s*-axis.

Step 3

Same measurements as in step 2 but now with $\alpha = 45°$.

Step 4

Measurement of I, $\langle r^2 \rangle$ and $\langle \eta^2 \rangle$ after the beam propagates successively through a quarter-wave plate (whose fast axis makes an angle 0° with the *s*-axis) and a polarizer with $\alpha = 45°$.

In terms of the experimental data, the traces of the matrices $\hat{S}_i$ are given by the following equations:

$$\mathrm{Tr}\, S_0 \;=\; 4\pi^2 \left(k^2 \langle r^2 \rangle_{FP} + \langle \eta^2 \rangle_{FP} \right) I_{FP}, \tag{2.60a}$$

$$\mathrm{Tr}\, S_1 \;=\; \frac{1}{T_1 - T_2} \left[8\pi^2 I_{0°} \left(k^2 \langle r^2 \rangle_{0°} + \langle \eta^2 \rangle_{0°} \right) - (T_1 + T_2)\, \mathrm{Tr}\hat{S}_0 \right], \tag{2.60b}$$

$$\mathrm{Tr}\, S_2 \;=\; \frac{1}{T_1 - T_2} \left[8\pi^2 I_{45°} \left(k^2 \langle r^2 \rangle_{45°} + \langle \eta^2 \rangle_{45°} \right) - (T_1 + T_2)\, \mathrm{Tr}\hat{S}_0 \right], \tag{2.60c}$$

$$\mathrm{Tr}\, S_3 = \frac{1}{T_1 - T_2} \left[\frac{8\pi^2 I_{\frac{\lambda}{4},45°}}{T_{\frac{\lambda}{4}}} \left(k^2 \langle r^2 \rangle_{\frac{\lambda}{4},45°} + \langle \eta^2 \rangle_{\frac{\lambda}{4},45°} \right) - (T_1 + T_2)\, \mathrm{Tr}\hat{S}_0 \right], \tag{2.60d}$$

where the subscript *FP* means free propagation, the coefficients T_1 and T_2 are the major and minor principal transmittances of the polarizer, $T_{\frac{\lambda}{4}}$ is the transmittance of the quarter-wave plate and the subscripts 0°, 45°, and $\frac{\lambda}{4}$,45° refer to the value of α and to the presence of the quarter-wave plate.

Method B

In this case the first steps measure the total power, the beam width and the divergence after the beam propagates through a polarizer oriented so as to transmit the component in the azimuths (i) $\alpha = 0°$; (ii) $\alpha = 45°$; (iii) $\alpha = 90°$ and (iv) $\alpha = 135°$. The same parameters are then measured after the beam travels successively through a quarter-wave plate whose fast-axis makes an angle 0° with the *s*-axis, and a polarizer with azimuth α=45° and $\alpha = 135°$; respectively. Again, the observation plane is not changed during the process.

The traces of the Stokes matrices now become

$$\mathrm{Tr}\, S_0 = \frac{4\pi^2}{T_1 + T_2}\left[I_{0^\circ}\left(k^2\langle r^2\rangle_{0^\circ} + \langle \eta^2\rangle_{0^\circ}\right) + I_{90^\circ}\left(k^2\langle r^2\rangle_{90^\circ} + \langle \eta^2\rangle_{90^\circ}\right)\right] \tag{2.61a}$$

$$\mathrm{Tr}\, S_1 = \frac{4\pi^2}{T_1 - T_2}\left[I_{0^\circ}\left(k^2\langle r^2\rangle_{0^\circ} + \langle \eta^2\rangle_{0^\circ}\right) - I_{90^\circ}\left(k^2\langle r^2\rangle_{90^\circ} + \langle \eta^2\rangle_{90^\circ}\right)\right], \tag{2.61b}$$

$$\begin{aligned}\mathrm{Tr}\, S_2 = \frac{4\pi^2}{T_1 - T_2}\Big[& I_{45^\circ}\left(k^2\langle r^2\rangle_{45^\circ} + \langle \eta^2\rangle_{45^\circ}\right) \\ & - I_{135^\circ}\left(k^2\langle r^2\rangle_{135^\circ} + \langle \eta^2\rangle_{135^\circ}\right)\Big]\end{aligned} \tag{2.61c}$$

$$\begin{aligned}\mathrm{Tr}\, S_3 = \frac{4\pi^2}{T_{\frac{\lambda}{4}}(T_1 - T_2)}\Big[& I_{\frac{\lambda}{4},45^\circ}\left(k^2\langle r^2\rangle_{\frac{\lambda}{4},45^\circ} + \langle \eta^2\rangle_{\frac{\lambda}{4},45^\circ}\right) \\ & - I_{\frac{\lambda}{4},135^\circ}\left(k^2\langle r^2\rangle_{\frac{\lambda}{4},135^\circ} + \langle \eta^2\rangle_{\frac{\lambda}{4},135^\circ}\right)\Big].\end{aligned} \tag{2.61d}$$

Let us finally remark that the main difference between the above methods arises from the existence in the former case of measurements of the direct, freely propagating beam, without using any polarizing elements, whereas, in method B, all measurements involve the presence of a polarizer.

Although the procedures are analytically simple, some care, however, is required because the optical devices are not ideal and may exhibit certain harmful effects.

For example, special attention should be taken to align the system in order that the beam crosses through the center of the optical components. Thus, when these components rotate, the influence of their spatial inhomogeneities on the overall irradiance will be strongly reduced. In an ideal configuration, note also that P_{G} should be independent of the angle formed by the polarization plane of the input beam (fixed all along the experiment) and the *s*-axis.

Let us finally remark that the polarizer could introduce some distortion into the beam irradiance profile. In particular, although the beam size of a uniformly polarized field should not change after crossing an ideal polarizer, however, in practice, the total irradiance reduction caused by the polarizer alters the beam width due to the influence of background and offset noises.

2.4.3 Generalized Degree of Polarization of Beams Emerging from Optically-Pumped Nd:YAG Rods

As an illustrative example, we will now determine the generalized degree of polarization of the field at the output of an optically pumped Nd:YAG rod. We will see that P_{G} could be a useful tool to infer the behavior of certain parameters of the system.

As is well known, the active medium in high-power solid-state laser resonators (for example, cylindrical rod in Nd:YAG lasers), involves thermal processes produced by both absorption of radiation and cooling. These thermal effects give rise to changes in the temperature, which exhibit a spatial dependence on the radial polar coordinate r (assuming homogeneous pumping in the laser rod). Moreover, birefringent mechanical strains are also induced by the temperature gradient.

In the particular case of high-power Nd:YAG lasers, the thermal processes generate a refractive index with a parabolic dependence on r. In other words, the laser rod behaves as a thin lens (thermal lens). In addition, the rod becomes birefringent with two values of the refractive index, n_r and n_ϕ, associated to light polarized along radial and azimuthal directions, respectively, (Lü et al., 1995)

$$n_r(r) = n_0\left(1 - \frac{\alpha_r}{2}r^2\right), \tag{2.62}$$

$$n_\varphi(r) = n_0\left(1 - \frac{\alpha_\varphi}{2}r^2\right), \tag{2.63}$$

n_0 being the refractive index at the center of the rod and α_r and α_ϕ being functions of a number of parameters, namely, the total power absorbed by the rod, the radius and the length of the rod, the thermal conductivity, and the photoelastic coefficients associated to the radial and azimuthal components.(Hodgson and Weber, 1993; Martínez-Herrero et al., 1995b; Montmerle et al., 2006)

Assuming well-collimated beams traveling along the rod, the birefringent medium may be modelled by a Jones matrix (referred to the Cartesian s and p axes):

$$\hat{\mathfrak{J}} = \begin{pmatrix} \mathfrak{J}_{ss}(r,\theta) & \mathfrak{J}_{sp}(r,\theta) \\ \mathfrak{J}_{sp}(r,\theta) & \mathfrak{J}_{pp}(r,\theta) \end{pmatrix}, \tag{2.64}$$

with

$$\mathfrak{J}_{ss}(r,\theta) = e^{ikLn_r(r)}\cos^2\theta + e^{ikLn_\varphi(r)}\sin^2\theta, \tag{2.65a}$$

$$\mathfrak{J}_{sp}(r,\theta) = \left[e^{ikLn_r(r)} - e^{ikLn_\varphi(r)}\right]\sin\theta\cos\theta, \tag{2.65b}$$

$$\mathfrak{J}_{pp}(r,\theta) = e^{ikLn_r(r)}\sin^2\theta + e^{ikLn_\varphi(r)}\cos^2\theta, \tag{2.65c}$$

where L is the length of the rod and the angle θ is shown in Fig. 2.8.

The active medium would then modify the polarization state of the input beam in a spatially non-uniform way. Note, however, that incident beams with radial or azimuthal linear polarization do not alter their polarization state after propagating through the rod.

For simplicity, let us now consider a typical linearly-polarized rotationally-symmetric Gaussian beam whose waist coincides with the entrance plane of the

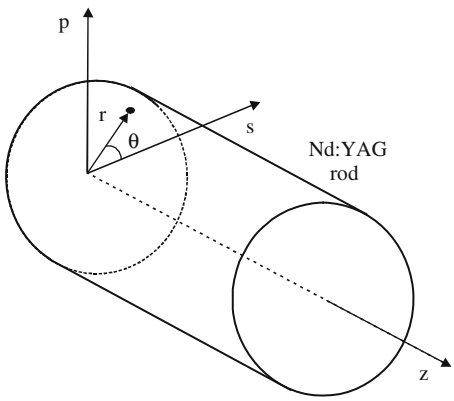

Fig. 2.8 Geometry and notation used to write the Jones matrix $\hat{\mathfrak{J}}$: r and θ denote polar coordinates at a plane orthogonal to the rod axis z

active medium. The amplitude of the electric field vector associated to such beam reads

$$\boldsymbol{E}\,(r,\theta) = E_0 \exp\left(-\frac{r^2}{w_0^2}\right)\begin{pmatrix}1\\0\end{pmatrix}, \tag{2.66}$$

where E_0 and w_0 are constants. By assuming the rod wide enough to neglect the border effects (diffraction and gain saturation effects are also ignored), the s- and p- components of the field at the output plane of de rod will then be obtained by applying the Jones matrix $\hat{\mathfrak{J}}$ to $\boldsymbol{E}\,(r,\theta)$, and one gets

$$E_s\,(r,\theta) = E_0\left[e^{ikLn_r(r)}\cos^2\theta + e^{ikLn_\varphi(r)}\sin^2\theta\right]\exp\left(-\frac{r^2}{w_0^2}\right), \tag{2.67a}$$

$$E_p\,(r,\theta) = E_0\sin\theta\cos\theta\left[e^{ikLn_\varphi(r)} - e^{ikLn_r(r)}\right]\exp\left(-\frac{r^2}{w_0^2}\right). \tag{2.67b}$$

From these equations, after lengthy but straightforward calculations, we find the following simple expression for the generalized degree of polarization at the output plane of the rod:

$$P_G = \frac{1}{2}\left[1 + \frac{1-\beta}{(1-\beta)^2}\right], \tag{2.68}$$

where the constant β contains information about the optical characteristics of the material, the beam size and the energy supplied to the medium (Movilla et al., 2000)

Equation (2.68) shows a one-to-one correspondence between P_G and β. Accordingly, the measurement of P_G would provide the value of β. The experimental set-up used to measure P_G is shown in Fig. 2.9, and P_G is plotted as a function of β in

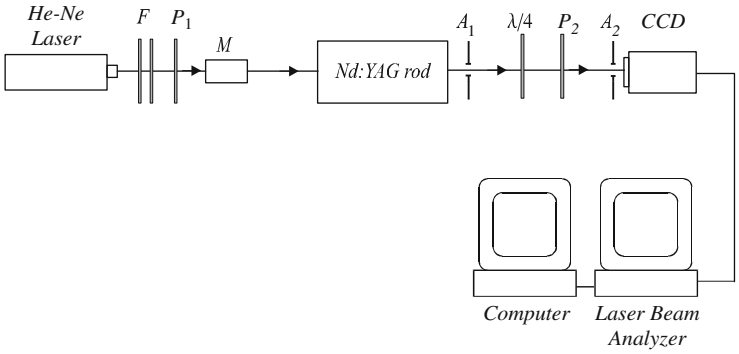

Fig. 2.9 Experimental setup used to measure the generalized degree of polarization, P_{G}, of an (initial) Gaussian beam crossing a birefringent optically-pumped Nd:YAG rod. *F* denotes neutral filters employed to attenuate the beam irradiance; P_1 represents a polarizer that controls the azimuth of the incident beam; *M* shows the presence of a magnifier $3\times$ that increases the beam size; A_1 and A_2 are two apertures to avoid that the light coming from the pumping lamps enter inside the detector; and finally $\lambda/4$ and P_2 symbolize the quarter-wave plate and the polarizer, respectively, that are used to determine the traces of the Stokes matrices. See also (Movilla et al., 2000)

Fig. 2.10. No experimental value appears in the central region of the curve because the beam size is not large enough to allow the accurate measurement of its width.

We see from Fig. 2.10 that the field essentially behaves as a uniformly polarized beam across its transversal section for low values of β. However, as β increases, the pumping produces non-uniform optical anisotropies inside the rod within the central regions, and the value of P_{G} reduces (non-uniform polarization distribution). Finally, P_{G} reaches a quasi-asymptotic behaviour for high pumping power, which means that depolarization is not complete. The same conclusion was also inferred by other authors analyzing a similar system (Kugler et al., 1997).

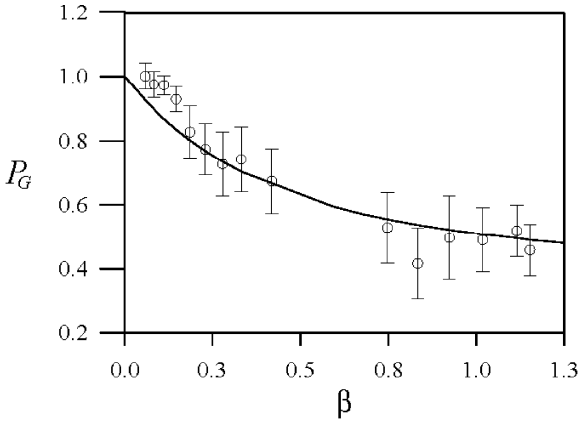

Fig. 2.10 P_{G} versus β. The circles are the experimental data and the continuos line plots the theoretical curve (cf. Eq.(2.68)) that best fits the experimental values. Ordinates include values greater than 1 because the experimental errors make P_G exceeds the limit value 1. See also (Movilla et al., 2000)

2.4.4 Classification Scheme of Partially Polarized Beams

The generalized degree of polarization, P_{G}, may be considered, in a sense, complementary to the parameters $\tilde{P}$ and $\tilde{\sigma}_p^2$ introduced in Chap. 1. To clarify this, let us again consider, for example, a radially polarized beam, whose polarization state is linear and oriented along radial lines from the beam axis. For these fields, $\tilde{P} = 1$ and $\tilde{\sigma}_p^2 = 0$, which are identical to the values associated to uniformly totally-polarized beams. To distinguish between both types of beams parameter P_{G} can be used: P_{G} equals zero for radially polarized fields but reaches its maximum value $P_{\mathrm{G}} = 1$ for uniformly totally polarized beams. Of course, in this example the radial polarization content can also be inferred from the parameters introduced in Sect. 1.5.

The triad of parameters P_{G}, $\tilde{P}$ and $\tilde{\sigma}_p^2$ provide, in addition, a global parametric characterization of the spatial distribution of the polarization state over the whole beam profile. On this basis, a rough but rather simple classification scheme of general (paraxial) partially polarized beams may formally be stated. Table 2.1 shows the sequence to be followed in order to classify a beam according with this scheme: thus, for example, the values $\tilde{\sigma}_p^2 = 0$, $\tilde{P} = 1$, $P_{\mathrm{G}} < 1$ would correspond to a non-uniformly totally polarized beam. We also see from Table 2.1 that, in certain cases, it is not necessary to determine all the three parameters.

Table 2.1 Classification scheme of partially polarized beams based on the parameters P_{G}, $\tilde{P}$ and $\tilde{\sigma}_{\mathrm{p}}^2$. The acronyms refer to the following types of fields: UP (uniformly polarized beams); UTP (uniformly totally polarized beams); UPP (uniformly partially polarized beams); NP (non-polarized beams); NUTP (non-uniformly totally polarized beams); NUPP (non-uniformly partially polarized beams)

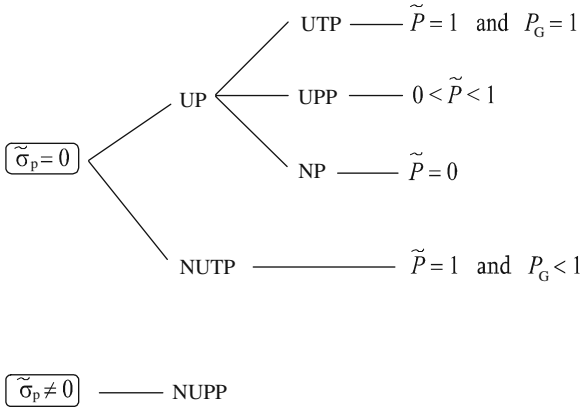

2.5 Beam Quality Parameter of Partially Polarized fields

In practice, it would be useful to handle a figure of merit providing a joint description of the focussing and collimation capabilities of a laser beam. To this purpose, the so-called beam quality parameter, Q, has been defined in the literature for partially-coherent scalar fields in terms of the second-order irradiance moments introduced in Sect. 2.2 (Lavi et al., 1988; Martínez-Herrero et al., 1992a, b; Martínez-Herrero and Mejías 1994; Mejías et al., 2002; Serna et al., 1991; Siegman, 1990, 1993a, b; Simon et al., 1988; Weber, 1992):

$$Q = \langle x^2 + y^2 \rangle \langle u^2 + v^2 \rangle - \langle xu + yv \rangle^2 = \langle r^2 \rangle \, \langle \eta^2 \rangle - \langle \boldsymbol{r} \cdot \boldsymbol{\eta} \rangle^2, \tag{2.69}$$

where, again, for simplicity, it has been assumed that $\langle x \rangle = \langle y \rangle = \langle u \rangle = \langle v \rangle = 0$. Since $\langle xu \rangle + \langle yv \rangle$ vanishes at the waist plane (see Sect. 2.2.1), the parameter Q can also be written in the form

$$Q = \langle r^2 \rangle_w \langle \eta^2 \rangle \tag{2.70}$$

where the subscript w means that the beam size is calculated at the waist plane. We thus see that this parameter contains simultaneous information of both the space and the spatial-frequency domains, characterizing the overall spatial structure of the beam at the near and at the far field. It should also be noticed that the squared root of Q is identical, a factor $k = 2\pi/\lambda$ apart, to the so-called beam propagation factor, M^2, introduced by Siegman (1990), namely,

$$M^2 = k\, Q^{1/2}. \tag{2.71}$$

The parameter Q exhibits two outstanding and practical properties:

(i) It remains invariant upon propagation through rotationally-symmetric first-order optical systems (even for beams without such symmetry and with non-zero crossed moments, $\langle xy \rangle$, $\langle xv \rangle$, $\langle yu \rangle$ or $\langle uv \rangle$).
(ii) It has a lower limit, given by the expression (uncertainty relation)

$$Q \geq 1/k^2, \tag{2.72}$$

or, equivalently,

$$M^2 \geq 1, \tag{2.73}$$

where the equalities are only reached by a Gaussian beam (best quality). It should also be remarked that the beam quality improves (better capabilities of the beam) when Q takes lower values, and, conversely, the quality deteriorates when the numerical value of Q increases.

These properties along with the simple measurement procedure explain why the beam propagation factor M^2 has been accepted as the current ISO beam quality standard (ISO, 1999, 2005).

A generalization of the quality parameter for the vectorial case can be achieved by extending, in a natural way, the former definition of Q, i.e., (Lü et al., 1995)

$$Q = \langle r^2 \rangle \langle \eta^2 \rangle - \langle \boldsymbol{r} \cdot \boldsymbol{\eta} \rangle^2, \tag{2.74}$$

where the second-order moments of the global vectorial beam now include both components, namely,

$$\langle r^2 \rangle = \frac{I_\mathrm{s}}{I} \langle r^2 \rangle_s + \frac{I_\mathrm{p}}{I} \langle r^2 \rangle_p, \tag{2.75}$$

$$\langle \eta^2 \rangle = \frac{I_s}{I} \langle \eta^2 \rangle_s + \frac{I_p}{I} \langle \eta^2 \rangle_p, \tag{2.76}$$

$$\langle \boldsymbol{r} \cdot \boldsymbol{\eta} \rangle = \frac{I_s}{I} \langle \boldsymbol{r} \cdot \boldsymbol{\eta} \rangle_\mathrm{s} + \frac{I_p}{I} \langle \boldsymbol{r} \cdot \boldsymbol{\eta} \rangle_\mathrm{p}, \tag{2.77}$$

In these equations

$$\langle \alpha\beta \rangle_i = \frac{1}{I_i} \frac{k^2}{4\pi^2} \iiint \alpha\beta \, \overline{E_i^* \, (\boldsymbol{r} + \boldsymbol{s}/2, z) \, E_i \, (\boldsymbol{r} - \boldsymbol{s}/2, z)} \exp(\mathrm{i} k \boldsymbol{s}.\boldsymbol{\eta}) \mathrm{d}\boldsymbol{s} \, \mathrm{d}\boldsymbol{r} \, \mathrm{d}\boldsymbol{\eta},$$

$$i = s, \, p; \quad \alpha, \beta = x, y, u, v \tag{2.78}$$

denote the second-order moments associated to the respective field components $I_\mathrm{i} = \iint \overline{|E_\mathrm{i}(\boldsymbol{r})|^2} \, d\boldsymbol{r}$, $i = \mathrm{s,p}$ and $I = I_\mathrm{s} + I_\mathrm{p}$. The presence of the factors I_i/I, $i = s$, p, arises from the different normalization constants (I and I_i) of the moments associated to the overall beam and to the field components, respectively. Note also that we are using sharp brackets to write the irradiance moments. Accordingly, $\boldsymbol{r} = (x, y)$ represents, as usual, the conventional position vector, with dimension of length.

As occurs in the scalar case, the parameter Q does not change when the beam freely propagates. Moreover, for any field, Q also satisfies the inequality

$$Q \geq 1/k^2, \tag{2.79}$$

where now the equality holds for uniformly totally-polarized Gaussian beams.

The parameter Q can also be written in terms of the beam qualities, Q_s and Q_p, associated to the electric field components. We have

$$Q = \left(\frac{I_s}{I} \right)^2 Q_s + \left(\frac{I_p}{I} \right)^2 Q_p + \left(\frac{I_s I_p}{I^2} \right) Q_{sp}, \tag{2.80}$$

where

$$Q_i = \langle r^2 \rangle_i \langle \eta^2 \rangle_i - \langle \boldsymbol{r} \cdot \boldsymbol{\eta} \rangle_i^2, i = s, p, \tag{2.81}$$

and

$$Q_{sp} = \langle r^2 \rangle_s \langle \eta^2 \rangle_p + \langle r^2 \rangle_p \langle \eta^2 \rangle_s - 2 \langle \boldsymbol{r} \cdot \boldsymbol{\eta} \rangle_s \langle \boldsymbol{r} \cdot \boldsymbol{\eta} \rangle_p, \tag{2.82}$$

For illustrative purposes, let us again consider the beam emerging from an optically pumped Nd:YAG rod (see the above section). It can be shown that the value of Q at the output plane of the rod is given by the simple formula (Lü et al., 1995; Mejías et al., 2002)

$$Q = \frac{1}{k^2} \left[1 + \beta + \ln(1 + \beta) \right]. \tag{2.83}$$

Accordingly, when β grows, the beam quality deteriorates. From the analytical expression of parameter β, it can be concluded that, in order to improve the beam quality of the output beam:

(i) the pumping power should decrease, and/or
(ii) the radius of the rod should increase, and/or
(iii) the transverse beam size should reduce.

This example shows how the beam quality parameter of the emerging field could be of simple practical use when designing laser devices.

2.6 Overall Parametric Characterization of PGSM Beams

We next apply the above parameters to provide a characterization of partially-polarized Gauss-Schell model (PGSM) beams, which were introduced in Chap. 1. More specifically, we investigate the behavior of the beam quality parameter and the different degrees of polarization (including P_G). For simplicity, the interest is focused on a particular class of PGSM beams, namely, those generated by PGSM sources that cannot be distinguished from ordinary GSM fields when polarization measurements are disregarded (i.e., when no anisotropic devices are inserted across the beam path).

Let us begin by writing the cross-spectral density matrix describing such fields at the waist plane (which takes a similar form to the corresponding BCP matrix)

$$\hat{W}(\boldsymbol{r}_1, \boldsymbol{r}_2) = \exp\left(-\frac{r_1^2 + r_2^2}{4\sigma^2} \right) \times \begin{pmatrix} A_s \exp\left[-\frac{(\boldsymbol{r}_1 - \boldsymbol{r}_2)^2}{2\mu^2} \right] & A_{sp} \exp\left[-\frac{(\boldsymbol{r}_1 - \boldsymbol{r}_2)^2}{2\mu_{sp}^2} \right] \\ A_{sp} \exp\left[-\frac{(\boldsymbol{r}_1 - \boldsymbol{r}_2)^2}{2\mu_{sp}^2} \right] & A_p \exp\left[-\frac{(\boldsymbol{r}_1 - \boldsymbol{r}_2)^2}{2\mu^2} \right] \end{pmatrix}, \tag{2.84}$$

where the parameters σ, μ, μ_{sp}, A_{s}, A_{p} and A_{sp} are analogous to those defined in Sect. 1.6. It should be remarked that they are linked through certain conditions derived from general properties of the cross-spectral density matrix (Gori et al., 2008).

For this kind of beams, the second-order irradiance moments become

$$\langle r^2\rangle = 2\langle r^2\rangle_s = 2\langle r^2\rangle_p = 2\langle r^2\rangle_{sp} = 2\sigma^2, \tag{2.85a}$$

$$\langle \eta^2\rangle = 2\langle \eta^2\rangle_s = 2\langle \eta^2\rangle_p = \frac{1}{2k^2\sigma^2\chi}, \tag{2.85b}$$

$$\langle \eta^2\rangle_{sp} = \frac{1}{4k^2\sigma^2\chi_{sp}}, \tag{2.85c}$$

where χ and χ_{sp} are given by the expressions

$$\frac{1}{\chi} = 4\sigma^2\left(\frac{1}{4\sigma^2} + \frac{1}{\mu^2}\right), \tag{2.86a}$$

$$\frac{1}{\chi_{sp}} = 4\sigma^2\left(\frac{1}{4\sigma^2} + \frac{1}{\mu_{sp}^2}\right), \tag{2.86b}$$

along with the condition $\chi_{sp} \geq \chi$. In Eqs. (2.85), the irradiance moments are defined by Eqs. (2.75), (2.76), (2.77), and (2.78), and

$$\langle r^2\rangle_{sp} = \frac{1}{I_{sp}}\frac{k^2}{4\pi^2}\iiint \left(x^2+y^2\right)\overline{E_s^*\left(\boldsymbol{r}+\boldsymbol{s}/2,z\right)E_p\left(\boldsymbol{r}-\boldsymbol{s}/2,z\right)}\exp\left(\mathrm{i}k\,\boldsymbol{s}\cdot\boldsymbol{\eta}\right)\mathrm{d}\boldsymbol{s}\,\mathrm{d}\boldsymbol{r}\,\mathrm{d}\boldsymbol{\eta}, \tag{2.87a}$$

$$\langle \eta^2\rangle_{sp} = \frac{1}{I_{sp}}\frac{k^2}{4\pi^2}\iiint \left(u^2+v^2\right)\overline{E_s^*\left(\boldsymbol{r}+\boldsymbol{s}/2,z\right)E_p\left(\boldsymbol{r}-\boldsymbol{s}/2,z\right)}\exp\left(\mathrm{i}k\,\boldsymbol{s}\cdot\boldsymbol{\eta}\right)\mathrm{d}\boldsymbol{s}\,\mathrm{d}\boldsymbol{r}\,\mathrm{d}\boldsymbol{\eta}, \tag{2.87b}$$

where

$$I_{sp} = \iint \overline{E_s(\boldsymbol{r})E_p^*(\boldsymbol{r})}\mathrm{d}\boldsymbol{r}. \tag{2.88}$$

Let us now introduce the quantity $\tilde{Q}_{sp}$ in the form

$$\tilde{Q}_{sp} = 4\langle r^2\rangle_{sp}\langle \eta^2\rangle_{sp}, \tag{2.89}$$

Note that $\tilde{Q}_{sp}$ involves the cross-correlation between the orthogonal s and p components of the field. No confusion should arise with regard to the function Q_{sp} given by Eq. (2.82), which did not consider any cross-correlation between components.

Both parameters, Q and $\tilde{Q}_{sp}$ are connected with the characteristic constants of the beam:

$$Q = \frac{1}{k^2 \chi}, \tag{2.90a}$$

$$\tilde{Q}_{sp} = \frac{1}{k^2 \chi_{sp}}, \tag{2.90b}$$

and satisfies $\tilde{Q}_{sp} \leq Q$ (remember that $\chi_{sp} \geq \chi$).

On the other hand, after some algebra, it can be shown that the standard degree of polarization of this class of fields turns out to be

$$P_{st} = \sqrt{\left(\frac{A_s - A_p}{A_s + A_p}\right)^2 + \frac{4A_{sp}^2}{\left(A_s + A_p\right)^2}}, \tag{2.91}$$

and, according with the equations given in Sect. 1.6, the local degree of polarization can be written in the form

$$P\left(\boldsymbol{r},z\right) = \sqrt{\left(\frac{A_s - A_p}{A_s + A_p}\right)^2 + \frac{4A_{sp}^2}{\left(A_s + A_p\right)^2} f^2\left(z\right) \exp\left[-a\left(z\right) r^2\right]},$$

where functions $f\left(z\right)$ and $a\left(z\right)$ are related with the spatial parameters Q and $\tilde{Q}_{sp}$ by the expressions

$$f\left(z\right) = \frac{4\sigma^4 + z^2 Q}{4\sigma^4 + z^2 \tilde{Q}_{sp}}, \tag{2.93a}$$

$$a\left(z\right) = \frac{4\sigma^2}{4\sigma^4 + z^2 Q}\left[f\left(z\right) - 1\right]. \tag{2.93b}$$

Note that function $f\left(z\right)$ increases as the beam propagates. In addition, its minimum value is reached at the waist plane, and we get

$$f\left(z = 0\right) = 1 \leq f\left(z\right) \leq f\left(z \to \infty\right) = \frac{Q}{\tilde{Q}_{sp}} = \frac{\chi_{sp}}{\chi}. \tag{2.94}$$

With regard to the generalized degree of polarization, P_G, it propagates for this type of beams according with the formula (Martínez-Herrero et al., 2004)

$$P_G\left(z\right) = \sqrt{\left(\frac{A_s - A_p}{A_s + A_p}\right)^2 + \frac{4A_{sp}^2}{\left(A_s + A_p\right)^2}\left(\frac{4\,k^2\sigma^4 + \frac{1}{k^2\chi_{sp}} + \frac{z^2}{\chi_{sp}}}{4\,k^2\sigma^4 + \frac{1}{k^2\chi} + \frac{z^2}{\chi}}\right)^2}. \tag{2.95}$$

We thus see that P_G decreases under free propagation, and for distances $z >> \lambda$ becomes

$$P_G(z) = \sqrt{\left(\frac{A_s - A_p}{A_s + A_p}\right)^2 + \frac{4A_{sp}^2}{\left(A_s + A_p\right)^2} \frac{1}{f^2(z)}}. \tag{2.96}$$

Close to the waist plane $z = 0$, the polarization parameters P_{st}, $P(0,z)$ and P_G are nearly identical for typical values of the beam parameters (width and divergence). Moreover, when $z >> \lambda$ (including the far field), the following relationship applies between the above three degrees of polarization:

$$\left[P_G^2(z) - \left(\frac{A_s - A_p}{A_s + A_p}\right)^2\right]\left[P^2(0,z) - \left(\frac{A_s - A_p}{A_s + A_p}\right)^2\right] = \left[P_{st}^2 - \left(\frac{A_s - A_p}{A_s + A_p}\right)^2\right]^2. \tag{2.97}$$

In particular, at the far-field they read

$$P_{st}(z \to \infty) = \sqrt{\left(\frac{A_s - A_p}{A_s + A_p}\right)^2 + \frac{4A_{sp}^2}{\left(A_s + A_p\right)^2}}, \tag{2.98a}$$

$$P(r, z \to \infty) = \sqrt{\left(\frac{A_s - A_p}{A_s + A_p}\right)^2 + \frac{4A_{sp}^2}{\left(A_s + A_p\right)^2}\left(\frac{Q}{\tilde{Q}_{sp}}\right)^2 \exp\left(-a_\infty r^2\right)}, \tag{2.98b}$$

$$P_G(z \to \infty) = \sqrt{\left(\frac{A_s - A_p}{A_s + A_p}\right)^2 + \frac{4A_{sp}^2}{\left(A_s + A_p\right)^2}\left(\frac{\tilde{Q}_{sp}}{Q}\right)^2}, \tag{2.98c}$$

where a_∞ represents the value of $a(z)$ at the far field.

For illustrative purposes, Fig. 2.11 computes the degrees of polarization $P_G(z)$, $P(\boldsymbol{r} = 0,z)$ and P_{st} in terms of the propagation distance z .

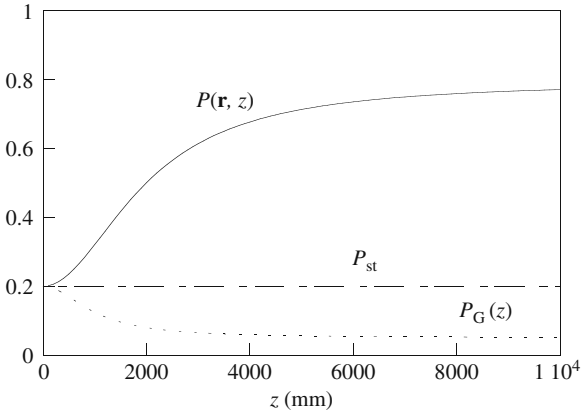

Fig. 2.11 Degrees of polarization $P(\boldsymbol{r} = 0,z)$, $P_G(z)$ and P_{st} versus the propagation distance z for a PGSM beam with the following characteristic parameters: $\sigma = 1$ mm. $\lambda = 633$ nm, $A_s = A_p = 0.5$, $A_{sp} = 0.1$, $\mu = 0.1$ mm and $\mu_{sp} = 0.2$ mm. In the figure, $P_{st} = 0.2$ (dotted line). See also (Martínez-Herrero et al., 2004)

To end this short survey, let us summarize a number of general properties derived for this class of beams:

(i) The local degree of polarization (squared) is a Gaussian function across the transverse profile (in accordance with previous theoretical and experimental results reported, for example, in (Gori et al., 2001; Piquero et al., 2002)).
(ii) Since the local and the generalized degree of polarization change upon free propagation according with the function $f(z)$, the overall polarization structure can then be determined at any plane z from the measurements of parameters Q and $\tilde{Q}_{sp}$ at the waist.
(iii) The parameters P_{st}, $P(\boldsymbol{r}=0,z)$, and $P_G(z)$ are nearly identical when $\mu_{sp} \sim \mu$.
(iv) If $A_{sp}^2 = A_s A_p$, then $P_{st} = P(\boldsymbol{r},z) = P_G(z) = 1$, and the beam is uniformly totally polarized at any transverse plane z.
(v) If $A_{sp} = 0$ then $P_{st} = P(\boldsymbol{r},z) = P_G(z) = \text{constant} < 1$. In other words, the beam is uniformly partially polarized. Moreover, for the particular case $A_s = A_p$, the three degrees of polarization,P_{st}, $P(\boldsymbol{r},z)$, and $P_G(z)$, are zero: The beam is unpolarized at every plane z.
(vi) If $A_s = A_p = A_0$ (as occurs in Fig. 2.11), the degrees of polarization are related at any plane z through the simple expression:

$$P_G(z)\,P(0,z) = P_{st}^2 = \frac{A_{sp}^2}{A_0^2}, \tag{2.99}$$

This means that the left-hand member of this equation is invariant upon free propagation, and it is also independent of the coherence characteristics of the field. In addition, we have in this case

$$\tilde{P} = P_{st} = \frac{A_{sp}}{A_0}, \tag{2.100}$$

and we see that the weighted degree of polarization (see Chap. 1) is independent of z as well. In particular, in Fig. 2.11 one has $\tilde{P} = P_{st} = 0.2$.

2.7 Beam Quality Improvement: General Considerations

Attention will now be devoted to the improvement of the beam quality parameter. Because of the invariance property of parameter Q in the scalar case, no rotationally-symmetric ABCD system could be employed to improve the quality of a partially coherent scalar beam. However, as it will next be apparent, such possibility arises when the vectorial behavior is taken into account. In the present section we will determine, for partially polarized beams, the optimized value of the beam quality parameter that can be attained by using rotationally-symmetric ABCD systems.

To begin with, note first that Q is invariant under rotation around the mean propagation direction. We can then choose, for convenience, a reference coordinate

system with respect to which

$$I_s = I_p \tag{2.101}$$

The angle θ between the new coordinate system and the former one is

$$\theta = \frac{1}{2}\left[\text{arctg}\left(\frac{I_s - I_p}{2\,\text{Re}\left\{I_{sp}\right\}}\right)\right], \tag{2.102}$$

where I_{sp} was defined in Eq. (2.88). In terms of this new coordinate system, the beam quality Q reads

$$Q = \frac{1}{4}\left(Q_s + Q_p + Q_{sp}\right). \tag{2.103}$$

Without loss of generality, let us assume, for simplicity, that the s-component reaches its waist at the plane where the irradiance moments are determined or measured. Accordingly, we can write at such plane.

$$\langle \boldsymbol{r} \cdot \boldsymbol{\eta} \rangle_s = 0, \tag{2.104}$$

and Q becomes

$$Q = \frac{1}{4}\left(Q_s + Q_p + \left\langle r^2 \right\rangle_s \left\langle \eta^2 \right\rangle_p + \left\langle r^2 \right\rangle_p \left\langle \eta^2 \right\rangle_s\right). \tag{2.105}$$

Let us now introduce the following functions (Martínez-Herrero et al., 2005):

$$F_1 = Q_s + \left\langle r^2 \right\rangle_s \left\langle \eta^2 \right\rangle_p, \tag{2.106}$$

$$F_2 = Q_p + \left\langle r^2 \right\rangle_p \left\langle \eta^2 \right\rangle_s, \tag{2.107}$$

Since Q_s, Q_p, $<r^2>_i$ and $<\eta^2>_i, i = s, p$, are positive quantities, we get

$$F_1 + F_2 \geq 2\sqrt{F_1 F_2}, \tag{2.108}$$

so that

$$Q \geq \frac{1}{2}\sqrt{F_1 F_2}, \tag{2.109}$$

In addition, functions F_1 and F_2 can be written in the form

$$F_i = G_i + J_i, \qquad i = 1,2, \tag{2.110}$$

with

$$G_1 = Q_s, \tag{2.111a}$$

$$J_1 = \left\langle r^2 \right\rangle_s \left\langle \eta^2 \right\rangle_p, \tag{2.111b}$$

$$G_2 = Q_p, \tag{2.111c}$$

$$J_2 = \left\langle r^2 \right\rangle_p \left\langle \eta^2 \right\rangle_s. \tag{2.111d}$$

Accordingly, we have

$$F_i = G_i + J_i \geq 2\sqrt{G_i J_i}, i = 1,2, \tag{2.112}$$

and therefore

$$Q^2 \geq \frac{1}{4} F_1 F_2 \geq \sqrt{G_1 J_1 G_2 J_2}. \tag{2.113}$$

Finally, since

$$\begin{aligned} G_1 J_1 G_2 J_2 &= Q_s Q_p \left\langle r^2 \right\rangle_s \left\langle \eta^2 \right\rangle_s \left\langle r^2 \right\rangle_p \left\langle \eta^2 \right\rangle_p = Q_s^2 Q_p \left\langle r^2 \right\rangle_p \left\langle \eta^2 \right\rangle_p \\ &\geq Q_s^2 Q_p \left(\left\langle r^2 \right\rangle_p \left\langle \eta^2 \right\rangle_p - \langle \boldsymbol{r} \cdot \boldsymbol{\eta} \rangle_p^2 \right) = Q_s^2 Q_p^2, \end{aligned} \tag{2.114}$$

it follows

$$Q^2 \geq Q_s Q_p. \tag{2.115}$$

This implies that the lower bound for the Q parameter of the partially polarized beam is the geometric mean of Q_s and Q_p. The equality is only reached when the second-order moments associated to each transverse field component are identical (recall we have chosen the coordinate system to make I_s equal to I_p). This, in turns, would imply that $Q_s = Q_p$.

We will next determine the lowest value of Q (best quality) that can be obtained by handling separate rotationally-symmetric first-order systems acting over each s- and p-component, along with the conditions to be fulfilled in order to optimize the overall beam quality (Martínez-Herrero et al., 2005).

The analysis is carried out by minimizing the function (see Eq. (2.115))

$$S(\chi, \beta) = 4\left[Q - \sqrt{Q_s Q_p} \right] = \left(\sqrt{Q_s} - \sqrt{Q_p} \right)^2 + \beta a + \chi b - 2\sqrt{Q_s Q_p}, \tag{2.116}$$

where

$$a \equiv \left\langle r^2 \right\rangle_s, \tag{2.117a}$$

$$b \equiv \left\langle \eta^2 \right\rangle_s, \tag{2.117b}$$

$$\chi \equiv \left\langle r^2 \right\rangle_p, \tag{2.117c}$$

$$\beta \equiv \left\langle \eta^2 \right\rangle_p. \tag{2.117d}$$

Note that

$$ab = Q_s \geq 1/k^2, \tag{2.118}$$

and

$$\chi\beta - \gamma^2 = Q_{\mathrm{p}} \geq 1/k^2, \tag{2.119}$$

where $\gamma = \langle \boldsymbol{r} \cdot \boldsymbol{\eta} \rangle_p$. In the calculations, we take a, b, Q_s and Q_p as known (measurable) parameters, and χ, β and γ as variables to be determined. Since they are linked through Eq. (2.119), the optimization procedure reduces to finding the minima of the following function

$$T(\chi,\gamma) = \left(\sqrt{Q_s} - \sqrt{Q_p}\right)^2 + \frac{a}{\chi}\left(Q_p + \gamma^2\right) + b\chi - 2\sqrt{Q_s Q_p} \tag{2.120}$$

Thus, by solving the equations

$$\frac{\partial T}{\partial \chi} = 0, \tag{2.121a}$$

$$\frac{\partial T}{\partial \gamma} = 0, \tag{2.121b}$$

we get that the critical points are given by

$$\chi_c = a\sqrt{Q_p/Q_s}, \tag{2.122}$$

$$\gamma_c = 0, \tag{2.123}$$

where the values χ_c, γ_c can be shown to represent a minimum of the function $T(\chi,\gamma)$. Equations (2.122) and (2.123) give the conditions to optimize the beam quality of the field. To get more insight into their physical meaning, let us write them in the more appropriate form

$$\left\langle r^2 \right\rangle_p = \left\langle r^2 \right\rangle_s \sqrt{Q_p/Q_s}, \tag{2.124}$$

$$\left\langle \eta^2 \right\rangle_p = \left\langle \eta^2 \right\rangle_s \sqrt{Q_p/Q_s}, \tag{2.125}$$

along with

$$\langle \boldsymbol{r} \cdot \boldsymbol{\eta} \rangle_p = 0. \tag{2.126}$$

Note that these three equations should be fulfilled at the plane where $\langle \boldsymbol{r} \cdot \boldsymbol{\eta} \rangle_s$ vanishes. They provide a precise relationship between the main second-order spatial parameters of the transverse field components. In addition, after substitution of Eqs. (2.124), (2.125), and (2.126) into Eq. (2.106), we find the optimized value of Q we are looking for:

$$(Q)_{optim} = \frac{1}{4}\left(\sqrt{Q_s} + \sqrt{Q_p}\right)^2. \tag{2.127}$$

Moreover, it can be shown at once that (Martínez-Herrero et al., 2005):

$$\min\left\{Q_s, Q_p\right\} \leq Q_{optim} \leq \max\left\{Q_s, Q_p\right\}, \tag{2.128}$$

i.e., Q_{optim} is always an intermediate value between Q_s and Q_p. Accordingly, when $Q_s = Q_p$, Q cannot be further improved: We have in such case (cf. Eqs. (2.124), (2.125), and (2.126))

$$\left\langle r^2 \right\rangle_p = \left\langle r^2 \right\rangle_s, \tag{2.129a}$$

$$\left\langle \eta^2 \right\rangle_p = \left\langle \eta^2 \right\rangle_s, \tag{2.129b}$$

$$\left\langle \boldsymbol{r} \cdot \boldsymbol{\eta}^2 \right\rangle_p = \left\langle \boldsymbol{r} \cdot \boldsymbol{\eta}^2 \right\rangle_s = 0, \tag{2.129c}$$

along with $I_s = I_p$ (see Eq. (2.101)).

In summary, the beam quality Q of the global field can be improved by means of rotationally-symmetric ABCD systems just to reach the value given by Eq. (2.127).

These conditions suggest a general procedure to optimize Q: the first two equalities (Eqs. (2.124) and (2.125)) show that the beam waists and divergences associated to the transverse field components should be exactly compensated, and Eq. (2.126) indicates that the waist planes of both components should match.

Taking this into account, a possible experimental scheme would involve a Mach-Zehnder-type (MZT) device, whose configuration resembles that of a classical Mach-Zehnder interferometer but now with a polarizer in each arm (Movilla et al., 2001). Thus, the field components can be controlled in a separate way in the optimization process.

For convenience, the transmission axes of the polarizers should match the reference coordinate system with respect to which $I_s = I_p$. Such a choice avoids interference between the emerging beams, because the transmission axes are then orthogonal.

To get the optimization conditions a two-step method can be followed: The initial beam can be made to propagate through a first MZT device with free propagation

paths in its arms in order to compensate for the different waist positions of the transverse beam components. The output of this interferometer is then made to travel through a second MZT arrangement that contains magnifiers to compensate for the corresponding beam sizes. Since a magnifier behaves as an ABCD optical system that increases the beam size, this also leads to a compensation for the difference in Rayleigh lengths z_{R} associated to each initial field components,

$$(z_R)_i = \left[\frac{\left(\langle r^2 \rangle_i\right)_w}{\langle \eta^2 \rangle_i} \right]^{1/2}, i = s,p, \tag{2.130}$$

where the subscript w refers to the waist plane. It should be pointed out that, when the waists of the field components are reached at the same plane, conditions (2.124) and (2.125) are met simultaneously.

To go further into the meaning of the optimization conditions, let us finally analyze two simple but general examples.

We first consider a beam whose moments associated to the s and p components are different but whose qualities Q_{s} and Q_{p} are identical. For simplicity, it is also assumed that $\langle \boldsymbol{r} \cdot \boldsymbol{\eta} \rangle_s = \langle \boldsymbol{r} \cdot \boldsymbol{\eta} \rangle_p = 0$. We then have

$$Q_s = \left\langle r^2 \right\rangle_s \left\langle \eta^2 \right\rangle_s = \left\langle r^2 \right\rangle_p \left\langle \eta^2 \right\rangle_p = Q_p \tag{2.131}$$

where $\langle r^2 \rangle_s \neq \langle r^2 \rangle_p$ and $\langle \eta^2 \rangle_s \neq \langle \eta^2 \rangle_p$. In this case, the global quality parameter Q reads

$$Q = \frac{Q_s}{4} \left(2 + q + \frac{1}{q} \right), \tag{2.132}$$

where

$$q \equiv \frac{\langle r^2 \rangle_s}{\langle r^2 \rangle_p} = \frac{\langle \eta^2 \rangle_p}{\langle \eta^2 \rangle_s}. \tag{2.133}$$

After using suitable MZT arrangements, we reach the optimized value

$$Q_{optim} = Q_s. \tag{2.134}$$

Remember that, in the present case, $Q_s = Q_p$. The relative quality improvement, $\Delta_{rel}Q$, defined in the form

$$\Delta_{rel}Q = \frac{Q - Q_{optim}}{Q}, \tag{2.135}$$

would then take the value

$$\Delta_{rel}Q = \frac{(1-q)^2}{(1+q)^2}. \tag{2.136}$$

In particular, when the second-order moments are identical, $q = 1$ so that $\Delta_{rel} Q = 0$. In the limit cases $q >> 1$ or $q << 1$ (very different beam sizes at the waist), we would get $\Delta_{rel} Q \approx 1$, which means strong beam quality improvement.

As a second example of interest, let us now focus our attention on those beams whose irradiance moments fulfil the relations

$$\langle r^2 \rangle_s = \langle r^2 \rangle_p, \tag{2.137a}$$

$$\langle \eta^2 \rangle_s \neq \langle \eta^2 \rangle_p, \tag{2.137b}$$

$$\langle \boldsymbol{r} \cdot \boldsymbol{\eta} \rangle_s = \langle \boldsymbol{r} \cdot \boldsymbol{\eta} \rangle_p = 0. \tag{2.137c}$$

It follows at once that $Q_s \neq Q_p$. Furthermore, the global quality parameter reads

$$Q = (1 + p) \frac{Q_s}{2}, \tag{2.138}$$

where

$$p \equiv \frac{\langle \eta^2 \rangle_p}{\langle \eta^2 \rangle_s}, \tag{2.139}$$

and the optimized value of Q becomes

$$Q_{optim} = (1 + p + 2\sqrt{p}) \frac{Q_s}{4}. \tag{2.140}$$

In this case we have

$$\Delta_{rel} Q = \frac{Q - Q_{optim}}{Q} = \frac{\left(1 - \sqrt{p}\right)^2}{2\,(1 + p)}. \tag{2.141}$$

For identical far-field divergences of the transverse field components (i.e., $p = 1$), it follows $\Delta_{rel} Q = 0$, as it should be expected. When the divergences drastically differ ($p >> 1$ or $p << 1$) then $\Delta_{rel} Q \approx 1/2$ which is half the change attained in the first example.

2.8 Beam Quality Improvement After Propagation Through Optical Phase Devices

In this section we investigate the influence of several optical devices on the quality parameter of light beams. More specifically, the possibility of beam quality improvement is examined when the field propagates through three kinds of phase components: Anisotropic pure-phase plates, quartic phase plates and spiral phase elements. It should be remarked that, due to the phase behavior of such

devices, no power losses would appear (in the ideal case) at the output of these components.

2.8.1 Propagation Through Anisotropic Pure-Phase Plates

Anisotropic pure-phase (APP) plates are analyzed in order to improve the quality parameter of an important class of partially coherent, partially polarized beams. In particular, we are interested on the determination of the phase transmittance of the APP plate that the beam should travel along to get the best quality keeping the same total power.

Within the framework of the paraxial approach, let us then consider a beam whose cross-spectral density matrix $\hat{W}$ contains diagonal elements of the form

$$\hat{W}_{ii}\left(\boldsymbol{r}_1,\boldsymbol{r}_2\right) = A_i\left(\boldsymbol{r}_1,\boldsymbol{r}_2\right)\exp\left\{i\left[\alpha_i\left(\boldsymbol{r}_2\right) - \alpha_i\left(\boldsymbol{r}_1\right)\right]\right\}, \; i = s,p, \tag{2.142}$$

where $\boldsymbol{r}_1$ and $\boldsymbol{r}_2$ are position vectors at a transverse plane, and A_i, α_i, i = s,p, are real functions, which should satisfy the relations

$$A_i\left(\boldsymbol{r}_1,\boldsymbol{r}_2\right) = A_i\left(\boldsymbol{r}_2,\boldsymbol{r}_1\right), \; i = s,p, \tag{2.143a}$$

$$A_i\left(\boldsymbol{r},\boldsymbol{r}\right) \geq 0, \; i = s,p, \tag{2.143b}$$

For simplicity, we will again choose our reference coordinate system in such a way that $I_s = I_p$, where now

$$I_i = \iint \hat{W}_{ii}(\boldsymbol{r},\boldsymbol{r})d\boldsymbol{r}, \quad i = s,p. \tag{2.144}$$

The class of fields we are considering includes those beams whose amplitude at any plane z can be written as an incoherent superposition of Hermite-Gauss modes. In particular, partially polarized Gaussian Schell-model sources belong to this family.

The APP plate can be represented, in the same reference system as before, by the Jones matrix

$$\hat{T}\left(\boldsymbol{r}\right) = \begin{pmatrix} \exp\left[i\Delta_s\left(\boldsymbol{r}\right)\right] & 0 \\ 0 & \exp\left[i\Delta_p\left(\boldsymbol{r}\right)\right] \end{pmatrix}. \tag{2.145}$$

Accordingly, the diagonal elements of $\hat{W}$ at the output of the APP plate are

$$\hat{W}_{ss}^{out}\left(\boldsymbol{r}_1,\boldsymbol{r}_2\right) = A_s\left(\boldsymbol{r}_1,\boldsymbol{r}_2\right)\exp\left\{i\left[\varphi_s\left(\boldsymbol{r}_2\right) - \varphi_s\left(\boldsymbol{r}_1\right)\right]\right\}, \tag{2.146a}$$

$$\hat{W}_{pp}^{out}\left(\boldsymbol{r}_1,\boldsymbol{r}_2\right) = A_p\left(\boldsymbol{r}_1,\boldsymbol{r}_2\right)\exp\left\{i\left[\varphi_p\left(\boldsymbol{r}_2\right) - \varphi_p\left(\boldsymbol{r}_1\right)\right]\right\}, \tag{2.146b}$$

where

$$\varphi_s(\boldsymbol{r}) = \alpha_s(\boldsymbol{r}) + \Delta_s(\boldsymbol{r}), \tag{2.147a}$$

$$\varphi_p(\boldsymbol{r}) = \alpha_p(\boldsymbol{r}) + \Delta_p(\boldsymbol{r}). \tag{2.147b}$$

Application of the definitions of the irradiance moments gives for the beam quality parameter Q^{out} at the output plane of the APP plate (Martínez-Herrero et al., 2003a)

$$Q^{out} = \langle r^2 \rangle G + F, \tag{2.148}$$

where $\langle r^2 \rangle$ is evaluated at the input plane,

$$\begin{aligned} G = \frac{1}{k^2 I}\Bigg[& \iint \left(\frac{\partial^2 A_s}{\partial x_1 \partial x_2} + \frac{\partial^2 A_s}{\partial y_1 \partial y_2} \right)_{x_1 = x_2 = x; y_1 = y_2 = y} dxdy + \\ & + \iint \left(\frac{\partial^2 A_p}{\partial x_1 \partial x_2} + \frac{\partial^2 A_p}{\partial y_1 \partial y_2} \right)_{x_1 = x_2 = x; y_1 = y_2 = y} dxdy \Bigg], \end{aligned} \tag{2.149}$$

is a function that depends only on the amplitude behavior of the input beam (therefore, G does not change after the APP plate), and

$$\begin{aligned} F = & \frac{\langle r^2 \rangle}{k^2 I} \left(\iint \left| \vec{\nabla} \varphi_s \right|^2 A_s dxdy + \iint \left| \vec{\nabla} \varphi_p \right|^2 A_p dxdy \right) \\ & - \left[\frac{1}{kI} \iint \left(\boldsymbol{r} \cdot \vec{\nabla} \varphi_s \right) A_s dxdy + \frac{1}{kI} \iint \left(\boldsymbol{r} . \vec{\nabla} \varphi_p \right) A_p dxdy \right]^2 \end{aligned} \tag{2.150}$$

It should be noted that the value of F involves information of both the phase of the input beam and the phase delay between the s and p components introduced by the plate. Furthermore, since the APP plate does not alter the value of G, the beam quality parameter at the output will depend only on F, which is always nonnegative (see (Martínez-Herrero et al., 2003a)). Accordingly, the best quality (lowest value of Q^{out}) will be obtained when $F = 0$. It can be shown (Martínez-Herrero et al., 2003a) that this occurs when

$$\alpha_s(\boldsymbol{r}) + \Delta_s(\boldsymbol{r}) = \alpha_p(\boldsymbol{r}) + \Delta_p(\boldsymbol{r}) = ar^2, \tag{2.151}$$

where a is a real-valued constant. In other words, for the beams we have considered here, the quality parameter would become optimized provided that either

(i) The phases of the s and p-components of the output field are identical, i.e., $a = 0$, or

(ii) The phase of the output field shows a quadratic dependence on the radial coordinate.

It should be noted that the quadratic phase factor $a\,r^2$ can be understood as the insertion of a lens (which does not change the quality parameter). Consequently, Eq. (2.151) indicates that, in order to optimize the quality, we have to remove the phase terms represented by the functions α_i, $i = s, p$. This is consistent with the results obtained in the previous section.

The physical meaning of Eq. (2.151) can be illustrated by means of a simple example: Let us consider a pure uniformly totally-polarized Gaussian beam propagating through a ground glass. The output field would belong to the type of beams studied here. The quality parameter of the output beam would be drastically affected by the action of the glass. To restore the original beam-quality value, it would obviously suffice to insert a plate that is phase conjugated with regard to the ground glass. But this is just what (2.151) shows.

In general, when the phase terms are completely removed, the APP plate behaves as a phase-conjugated filter (Pepper, 1985) matched to the phase transmittance of the light field. Equation (2.151) then assures that the quality parameter of the output field has the highest quality one can get by using pure-phase transmittances.

2.8.2 *Propagation of Radially and Azimuthally Polarized Beams Through Quartic Phase Plates*

We now analyze the change suffered by the beam quality of a radially (or azimuthally) polarized field, caused by quartic phase distortions, as occurs, for example, in strongly pumped laser rods used in high-power solid-state lasers (see Sect. 2.4).

For the sake of convenience, we will use planar polar coordinates, r and θ. The transverse field would then read

$$\boldsymbol{E}(r,\theta) = \left(E_s(r,\theta), E_p(r,\theta)\right), \tag{2.152}$$

and the electric field amplitude of a coherent radially (or azimuthally) polarized beam becomes

$$\boldsymbol{E}_R(r,\theta) = f(r)\,(\cos\theta, \sin\theta)\,, \tag{2.153a}$$

$$\boldsymbol{E}_\theta(r,\theta) = f(r)\,(-\sin\theta, \cos\theta)\,, \tag{2.153b}$$

where the subscripts R and θ stand for radial and azimuthal polarization, respectively. For both types of fields, the powers associated with the transverse

components are identical. Furthermore, the overall second-order moments are given by

$$\langle r^2 \rangle = \frac{1}{P} \int_0^\infty r^2 \, |f(r)|^2 \, r \, dr, \tag{2.154a}$$

$$\langle \eta^2 \rangle = \frac{1}{k^2 P} \int_0^\infty \left(\left| \frac{df}{dr} \right|^2 + \frac{1}{r^2} \, |f(r)|^2 \right) r \, dr, \tag{2.154b}$$

$$\langle \boldsymbol{r} \cdot \boldsymbol{\eta} \rangle = \frac{1}{2i \, k \, P} \int_0^\infty r \left(f^* \frac{df}{dr} - f \frac{df^*}{dr} \right) r \, dr, \tag{2.154c}$$

where

$$P = \int_0^\infty |f(r)|^2 \, r \, dr \tag{2.155}$$

Note that the above expressions do not depend on the coordinate θ. Let us now compare these formulae with the corresponding equations for *scalar* fields rotationally-symmetric around the z-axis. It should be remarked that, in the scalar case, we have to apply the scalar definition of the beam quality parameter (Lavi et al., 1988; Martínez-Herrero et al., 1992a, b; Siegman, 1990, 1993a, b; Simon et al., 1988; Serna et al., 1991; Weber, 1992). It can be shown that the only but important difference between both cases arises from the term $|f|^2/r^2$ in Eq. (2.154b). More specifically,

$$Q_{vectorial} = Q_{scalar} + \langle r^2 \rangle \, g, \tag{2.156}$$

where

$$g = \frac{1}{k^2 P} \int_0^\infty \frac{|f(r)|^2}{r^2} r \, dr. \tag{2.157}$$

We see that the second term of the right-hand side of Eq. (2.156) does not appear in the scalar case. Since this term is positive, it then follows that the value of the vectorial beam quality is always greater than the corresponding value of the scalar parameter.

Let us now consider that the radially (or azimuthally) polarized beam propagates through a strongly pumped laser rod. For the sake of simplicity, we assume in the calculations that changes in the beam diameter along the rod are not significant (this is the same assumption accepted in Sect. 2.4).

We know that, at high pump power, combined thermal lensing and birefringence generate a spherically aberrated lens, or, equivalently, an induced phase plate, $\exp[ik\Delta(r)]$ with

$$\Delta(r) = \alpha \frac{r^2}{2} + \beta \frac{r^4}{4}, \tag{2.158}$$

where α and β are, respectively, the quadratic and quartic coefficients describing the physical characteristics of the global process (Montmerle et al., 2006). Note that the values of α and β depend on the polarization of the incident field (radial or azimuthal): The low-order spherical aberration (SA) can be strongly reduced by using non-homogeneous pumping distribution. However, when the low-order SA vanishes, high-order spherical aberrations could rapidly increase. Consequently, in terms of beam quality preservation, a compromise should be established between low and high-order SA.

Here our interest is focused on the beam quality changes generated by the quartic term of Eq. (2.158). It can be found that the increment ΔQ, induced by SA, is given by

$$\Delta Q = Q_{out} - Q_{inp} = 2\beta \left(A \langle r^2 \rangle - \langle r^4 \rangle \langle \boldsymbol{r} \cdot \boldsymbol{\eta} \rangle \right) + \beta^2 \left(\langle r^2 \rangle \langle r^6 \rangle - \langle r^4 \rangle^2 \right), \tag{2.159}$$

where the subscripts *inp* and *out* refer to the input and output values of Q before and after crossing the rod, and

$$\langle r^n \rangle = \frac{1}{P} \int_0^\infty r^n \, |f(r)|^2 \, r \, dr, \quad n = 2,4,6 \tag{2.160}$$

$$A = \frac{i}{2kP} \int_0^\infty r^3 \left(f \frac{df^*}{dr} - f^* \frac{df}{dr} \right) r \, dr. \tag{2.161}$$

The sign of ΔQ (i.e., degradation or improvement of the beam quality) would depend on the spatial shape of the irradiance profile of the propagating beam. It should also be noted that the second term of the right-hand side of Eq. (2.159) is positive for every $f(r)$, whereas the sign of the first term depends on both, the transverse irradiance and the phase distribution of the output field.

Comparison between the beam quality change in the scalar and vectorial cases, shows that ΔQ is the same for both, rotationally-symmetric scalar beams and radially (or azimuthally) polarized fields. It should, however, be remarked that the ratio $\Delta Q/Q$ differs: In fact,

$$\left(\frac{\Delta Q}{Q} \right)_{vectorial} < \left(\frac{\Delta Q}{Q} \right)_{scalar}. \tag{2.162}$$

The above analysis can be illustrated by means of two simple examples. Let us first consider a radially or azimuthally polarized beam whose input amplitude $f(r)$ reads

$$f(r) = f_0(r)\,\exp\left(ikbr^2\right), \tag{2.163}$$

where b and f_0 are real quantities. In particular, beams whose amplitude is written in the form (Deng, 2006; Zhou, 2006)

$$f_{0n}(r) = r\,L_n^1\left(\frac{2r^2}{\omega_0^2}\right)\exp\left(-\frac{r^2}{\omega_0^2}\right), n = 1,2\ldots., \tag{2.164}$$

belong to this family (L_n^1 denoting the generalized Laguerre polynomials (Siegman, 1986)). For such fields we obtain (Martínez-Herrero et al., 2008)

$$\langle \boldsymbol{r}\cdot\boldsymbol{\eta}\rangle = 2\,b\,\langle r^2\rangle, \tag{2.165a}$$

$$A = 2\,b\,\langle r^4\rangle, \tag{2.165b}$$

and ΔQ reduces to

$$\Delta Q = \beta^2\left(\langle r^2\rangle\langle r^6\rangle - \langle r^4\rangle^2\right). \tag{2.166}$$

But ΔQ is positive. Consequently, for this kind of fields, the beam quality will always be degraded after passing through highly pumped laser rods. Figure 2.12 illustrates that the value ΔQ strongly increases for high values of the order n.

Let us finally write ΔQ in the form

$$\Delta Q = \frac{16}{k^2}\left(\frac{k\beta\langle r^2\rangle^2}{4}\right)^2\left[\frac{\langle r^6\rangle}{\langle r^2\rangle^3} - \left(\frac{\langle r^4\rangle}{\langle r^2\rangle^2}\right)^2\right]. \tag{2.167}$$

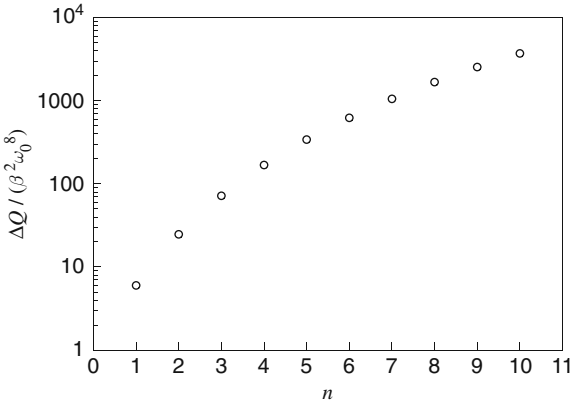

Fig. 2.12 Dimensionless ratio $\left(\Delta Q/\beta^2\omega_0^8\right)$ for the set of radially (or azimuthally) polarized beams whose amplitude is given by Eq. (2.164). The abscisses show the order n of the generalized Laguerre polynomials L_n^1. See also (Martínez-Herrero et al., 2008)

Since the factor $(k\beta\langle r^2\rangle^2/4)$ closely resembles the quartic phase term, we see that this factor explicitly shows the influence of the spherical aberration on the beam quality degradation.

As a second example we now consider a radially (or azimuthally) polarized beam whose incident amplitude $f(r)$ reads

$$f(r) = [I(r)]^{1/2} \exp\left[i\, k\varphi(r)\right], \tag{2.168}$$

where

$$\varphi(r) = \frac{ar^4}{4} + \frac{br^2}{2}, \tag{2.169}$$

and $I(r)$ denotes the irradiance. Equation (2.161) now becomes

$$A = \frac{1}{P} \int_0^\infty r^3 \frac{d\varphi(r)}{dr} I(r)\, r\, dr, \tag{2.170}$$

along with

$$\langle \boldsymbol{r} \cdot \boldsymbol{\eta} \rangle = \frac{1}{P} \int_0^\infty r \frac{d\varphi(r)}{dr} I(r)\, r\, dr. \tag{2.171}$$

After simple calculations, we obtain

$$\Delta Q = \left(\langle r^6\rangle\langle r^2\rangle - \langle r^4\rangle^2\right)\left(2\beta a + \beta^2\right). \tag{2.172}$$

Two conclusions can finally be derived from this expression:

(i) When $a = 0$ (as occurs in the above Laguerre-Gauss example), we have $\Delta Q > 0$, for any b and $I(r)$.
(ii) When $a = -\beta$, we then get $\Delta Q < 0$, for any b and $I(r)$. In other words, for this kind of polarized beams, a quartic phase plate could improve the beam quality.

2.8.3 Propagation Through Spiral Phase Elements

Attention will now be focused on the so-called spiral phase elements (SPEs) (Machavariani et al., 2007; Niv et al., 2005; Oemrawsingh et al., 2004; Oron et al., 2000; Xie and Zhao, 2008). The increasing interest on this kind of optical devices arises from their use in connection with certain depleted-center beams employed in a number of applications (Kuga et al., 1997; McCelland and Scheinfein, 1991; Molina-Terriza et al., 2007; Sato et al., 1994; Torner et al., 2005) such as, for instance, trapping of microscopic particles, focusing of atomic beams, and digital

spiral imaging, all of them well described in certain cases by means of the spiral spectrum of the light field.

We will next provide an introductory analysis about the changes suffered by the beam quality parameter of partially polarized, partially coherent fields travelling along SPEs.

The so-called spiral spectrum of a beam has revealed to be a useful tool to handle some type of situations. Let us introduce the spiral spectrum decomposition of the vector $\boldsymbol{E}(R,\theta)$ at a transverse plane (say, $z = 0$) in the form

$$\boldsymbol{E}(R,\theta) = \sum_n \boldsymbol{E}_n(R)\exp(in\theta), \tag{2.173}$$

where R and θ denote the planar polar coordinates, and

$$\boldsymbol{E}_n(R) = \frac{1}{2\pi}\int_0^{2\pi} \boldsymbol{E}(R,\theta)\exp(-in\theta)d\theta. \tag{2.174}$$

As in the previous section, for the sake of simplicity, we again choose the s- and p-axis in such a way that $I_s = I_p = I$.

By using Eq. (2.173), we get that the main second-order irradiance moments of a light beam can be written in terms of its spiral spectrum as follows (Martínez-Herrero and Manjavacas, 2009)

$$\left\langle r^2\right\rangle = \frac{\pi}{I}\sum_n \int_0^\infty \overline{|\boldsymbol{E}_n(R)|^2}R^3 dR, \tag{2.175a}$$

$$\left\langle \eta^2\right\rangle = \frac{\pi}{k^2 I}\sum_n \int_0^\infty \overline{\left|\boldsymbol{E}_n'(R)\right|^2}RdR + \frac{\pi}{k^2 I}\sum_n n^2\int_0^\infty \overline{|\boldsymbol{E}_n(R)|^2}\frac{1}{R}dR, \tag{2.175b}$$

$$\begin{aligned}\langle \boldsymbol{r}\cdot\boldsymbol{\eta}\rangle = \frac{\pi}{ikI}\sum_n \int_0^\infty \Big[&\overline{E_{ns}'(R)E_{ns}^*(R) - E_{ns}'^*(R)E_{ns}(R)} \\ &+ \overline{E_{np}'(R)E_{np}^*(R) - E_{np}'^*(R)E_{np}(R)}\Big]RdR\end{aligned} \tag{2.175c}$$

where the prime means derivation with respect to R. Application of Eq. (2.175b) requires that the irradiance of the field on the propagation axis decays with R^{m}, with $\mathrm{m} > 1$. Otherwise, the far-field moment $< \eta^2 >$ diverges. This comes from the singularity in the center, $R = 0$. It is also clear from these equations that the second-order moments can be understood as the sum of the corresponding moments associated to the spiral spectrum components.

Let us now assume that the light beam passes through a spiral phase element. This device will add a spiral phase $\varphi = p\theta$ to the field amplitude. Accordingly, the above irradiance moments at the input and output planes of the SPE are linked by

the following equations:

$$\left\langle r^2 \right\rangle_{out} = \left\langle r^2 \right\rangle_{inp}, \tag{2.176a}$$

$$\langle \boldsymbol{r} \cdot \boldsymbol{\eta} \rangle_{out} = \langle \boldsymbol{r} \cdot \boldsymbol{\eta} \rangle_{inp}, \tag{2.176b}$$

$$\left\langle \eta^2 \right\rangle_{out} = \left\langle \eta^2 \right\rangle_{inp} + M_p, \tag{2.176c}$$

where

$$M_p = \frac{\pi}{k^2 I} \sum_n \left(p^2 + 2np \right) \int_0^\infty \overline{|\mathbf{E}_n(R)|^2} \frac{1}{R} dR. \tag{2.177}$$

As expected, the beam width and the average curvature radii remain unchanged. However, the SPE alters the far-field divergence. Moreover, since the SPE introduces a change on the spiral spectrum of the field, the polarization behavior is also modified upon free propagation.

In addition, the output quality parameter, Q_{out}, reads

$$Q_{out} = Q_{inp} + \left\langle r^2 \right\rangle_{inp} M_p \tag{2.178}$$

Taking this into account, we finally obtain for the ratio $\frac{Q_{out} - Q_{inp}}{Q_{inp}}$ the value

$$\frac{\Delta Q}{Q_i} \equiv \frac{Q_{out} - Q_{inp}}{Q_{inp}} = \frac{\left\langle r^2 \right\rangle_{inp} M_p}{Q_{inp}}. \tag{2.179}$$

We thus conclude that, depending on the characteristics of the spiral spectrum of the specific light field, the SPE could improve or deteriorate the beam quality parameter. Here we do not proceed further into this subject, which deserves more study in the future. Application to some examples of interest can be found, for instance, in (Martínez-Herrero and Manjavacas, 2009).

2.9 Global Beam Shaping with Non-uniformly Polarized Beams

As is well known, in a number of applications one needs to obtain a prescribed beam profile at a certain transverse plane. Consequently, optical devices should be designed in order to modify at will the irradiance distributions of the laser beam. Drilling, welding, surface treatment, laser fusion experiments, information recording or optical data processing are examples in which appropriate transversal profiles are required.

This topic, namely, the implementation of particular distributions of irradiance (beam shaping) has been extensively investigated in the literature, and a large number of methods have been reported. They are based on refraction, reflection of beams over prescribed surfaces, diffraction, absorption, and transmission through pure phase plates or liquid-crystal layers, to mention only some of them. The majority of these techniques have been studied within the framework of the scalar theory of light, without taking into account its vectorial nature. Comparatively, there are not many papers that consider the polarization properties for beam shaping. In such cases, the techniques were focused on modifying the irradiance distribution at each point of the transverse section of the beam.

Here we consider a different approach, based on the global parameters introduced in this chapter. In fact, we are interested on a global shaping, which involves the control of the overall characteristics of the light field. For illustrative purposes, in the present section we show a simple example of application. Attention will be restricted on two parameters, the beam quality and the so-called kurtosis (Amarande, 1996; Martínez-Herrero et al., 1995a; Martínez-Herrero and Mejías 1997a), associated to the sharpness of the beam profile. To modify these parameters, several optical devices have already been proposed, such as binary phase plates (Siegman, 1993b), quartic phase plates (Martínez-Herrero et al., 1992b, Martínez-Herrero and Mejías 1993a; Siegman, 1993a), aberrated lenses (Alda et al., 1997; Piquero et al., 1994) and axicons (Luo and Lu, 2003). Next we briefly analyze a procedure that takes the vectorial character of light into account.

The method is essentially based on the generation of a non-uniformly totally polarized field by means of a Mach-Zehnder-type interferometric system.

To begin with, let us assume a beamlike field propagating along the z-axis. For the sake of simplicity, we consider in this example the two-dimensional x-z case, i.e., we write the field components as follows

$$\boldsymbol{E}(x,z) = \left(E_s(x,z),E_p(x,z)\right). \tag{2.180}$$

The so-called kurtosis parameter, K, is then defined in terms of higher-order irradiance moments in the form (Martínez-Herrero et al., 1995a)

$$K = \frac{\langle x^4 \rangle}{\langle x^2 \rangle^2} \tag{2.181}$$

with

$$\langle x^n \rangle = \frac{I_s}{I} \langle x^n \rangle_s + \frac{I_p}{I} \langle x^n \rangle_p \ ; n = 2,4, \tag{2.182}$$

where I_s, I_p and I were defined earlier. This parameter provides information about the sharpness or flatness of the beam profile. As a matter of fact, any beam can be classified as leptokurtic ($K > 3$), platykurtic ($K < 3$) or mesokurtic ($K = 3$). Since the kurtosis value of a Gaussian beam equals 3, leptokurtic and platykurtic profiles

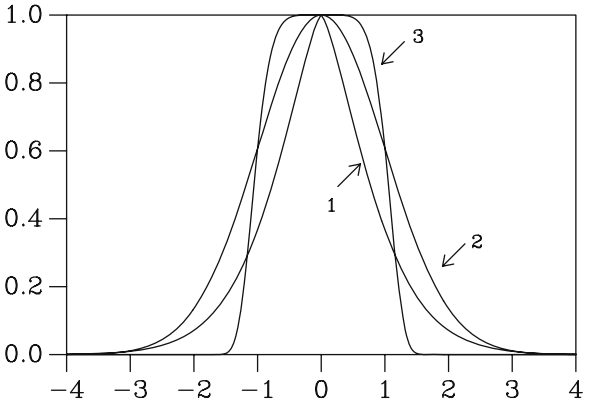

Fig. 2.13 Plots of three kinds of functions with regard to their values of the kurtosis: (*1*) leptokurtic ($K > 3$); (*2*) mesokurtic ($K = 3$); and (*3*) platykurtic ($K < 3$)

imply (globally) sharper and flatter beams, respectively, than the Gaussian case (see Fig. 2.13).

Let us now consider a Mach-Zehnder-type arrangement, in which two different amplitude filters are placed at each arm of the interferometer (see Fig. 2.14).

The transmittances of the filters are chosen to be the functions

$$t_i(x) = \exp\left[-g_i(x)\right], i = 1{,}2, \tag{2.183}$$

where $g_i(x)$, $i = 1{,}2$, denote the real-valued functions

$$g_1(x) = \frac{1}{2}\,(a\,x)^{2m}\,, \tag{2.184a}$$

and

$$g_2(x) = \frac{1}{2}\,(b\,x)^{2n}\,, \tag{2.184b}$$

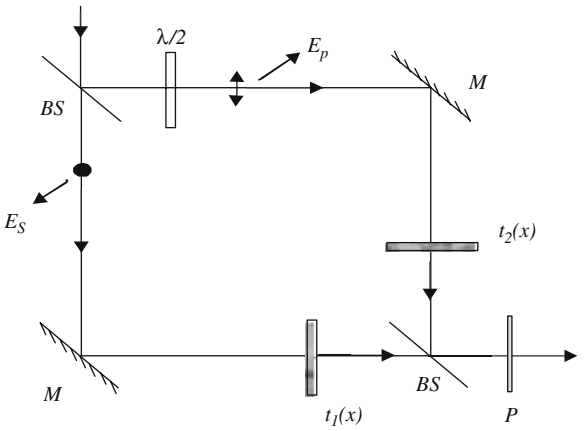

Fig. 2.14 Interferometric setup for global beam shaping. E_S and E_P are the field components of the beam, orthogonal to the propagation direction, λ/2 is a suitably rotated half-wave plate used to get the p-component, $t_1(x)$ and $t_2(x)$ are the amplitude transmittances, *M* denotes the mirrors, *BS* indicates the position of the beam splitters of the Mach-Zehnder arrangement, and *P* represents the linear polarizer that controls the parameters *Q* and *K* of the output beam

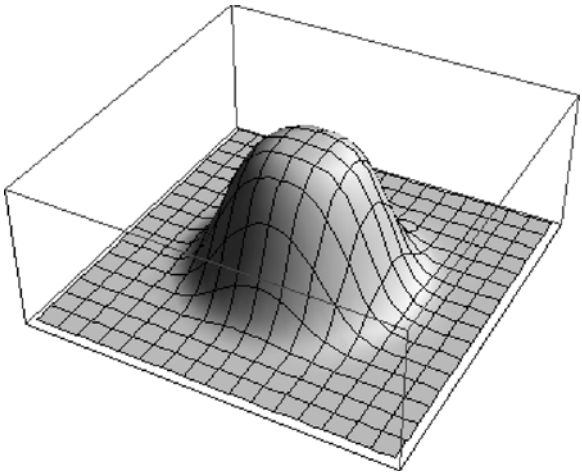

Fig. 2.15 Plot of a superGaussian transmittance (3D case) for $n = 2$

a and b being positive constants related to the aperture widths, and n and m are positive integers. As is well known, when n,$m > 1$ the transmittances are super-Gaussian functions. In such case, diffraction effects are expected to be negligible enough because these filters should be considered as soft-edge apertures (see, for example, Fig. 2.15).

If, for simplicity, the incident beam on the MZT device is assumed to be a plane wave, linearly polarized along the s-axis, it can be shown (Ramírez-Sánchez and Piquero, 2006) that the beam quality, Q, and the kurtosis parameter of the beam at the output of the interferometer (just before the polarizer P) read

$$Q = \frac{1}{2\,k^2}\left[ma\,\Gamma\left(2-\frac{1}{2m}\right)+n\,b\,\Gamma\left(2-\frac{1}{2n}\right)\right]\frac{\left[\frac{a^{-3}}{m}\Gamma\left(\frac{3}{2m}\right)+\frac{b^{-3}}{n}\Gamma\left(\frac{3}{2n}\right)\right]}{\left[\frac{a^{-1}}{m}\Gamma\left(\frac{1}{2m}\right)+\frac{b^{-1}}{n}\Gamma\left(\frac{1}{2n}\right)\right]^2}, \tag{2.185}$$

$$K = \left[\frac{a^{-1}}{2m}\Gamma\left(\frac{1}{2m}\right)+\frac{b^{-1}}{2n}\Gamma\left(\frac{1}{2n}\right)\right]\frac{\left[\frac{a^{-5}}{m}\Gamma\left(\frac{5}{2m}\right)+\frac{b^{-5}}{n}\Gamma\left(\frac{5}{2n}\right)\right]}{\left[\frac{a^{-3}}{m}\Gamma\left(\frac{3}{2m}\right)+\frac{b^{-3}}{n}\Gamma\left(\frac{3}{2n}\right)\right]^2}, \tag{2.186}$$

where Γ denotes the gamma function. From these expressions, it follows that the minimum value of Q (optimized quality) is reached when $a = b$ and $m = n$, as it should be expected. In such a case, throughout the wavefront, the output beam is linearly polarized with azimuth 45°.

In order to modify, in a continuous and controlled way, the parameters Q and K, a dichroic linear polarizer can be placed at the output plane of the MZT system. For different angles θ between the transmission axis of the polarizer and the x-axis, a global beam shaping can be implemented. In particular, when θ is equal to 0° or 90°, Q and K do not depend on the widths a and b, as expected. In such cases,

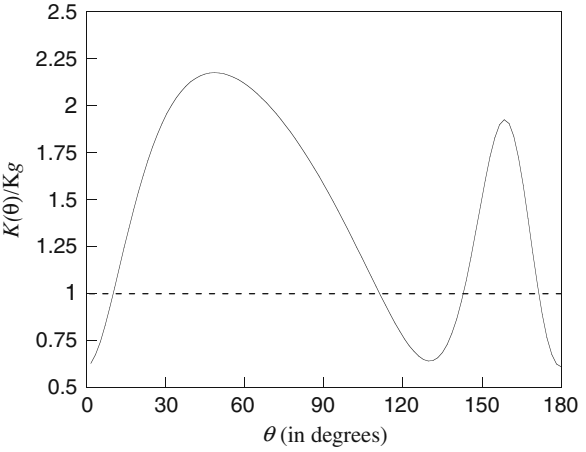

Fig. 2.16 Ratio K/K_g after the polarizer (at the output of the Mach-Zehnder arrangement) versus the angle θ that defines the orientation of the transmission axis of P. See also (Ramírez-Sánchez and Piquero, 2006)

the analytical expressions for the beam quality and the kurtosis at the output of the polarizer take the following simple forms:

$$Q = \frac{n^2}{k^2} \frac{\Gamma(3/2n)\Gamma(2 - 1/2n)}{\Gamma^2(1/2n)}, \tag{2.187}$$

$$K = \frac{\Gamma(5/2n)\Gamma(1/2n)}{\Gamma^2(3/2n)}. \tag{2.188}$$

Figure 2.16 computes the ratio K/K_g versus the angle θ, for the values $n = 0.6$, $m = 10$ and $a = b = 1$ mm^{-1}, K_g being the kurtosis of a Gaussian beam ($K_g = 3$). In this figure, the ratio ranges from 0.61 to 2.17, and the kurtosis exhibits maxima and minima. This means that the overall beam profile changes from leptokurtic to platykurtic and viceversa, becoming sharper or flatter depending on the orientation of the polarizer.

References

Abramochkin, E., Losevsky, N., Volostnikov, V. (1997): Generation of spiral-type laser beams, Opt. Commun. 141, 59–64.

Alda, J., Alonso, J., Bernabeu, E. (1997): Characterization of aberrated laser beams, J. Opt. Soc. Am. A 14, 2737–2747.

Alieva, T., Bastiaans, M. J. (2004): Evolution of the vortex and the asymmetrical parts of orbital angular momentum in separable first-order optical systems, Opt. Lett. 29, 1587–1589.

Allen, L., Padgett, M. J., Babiker, M. (1999): The orbital angular momentum of light, Prog. Opt. 39, 291-372.

Amarande, S. A. (1996): Beam propagation factor and the kurtosis parameter of flattened Gaussian beams, Opt. Commun. 129, 311–317.

Bastiaans, M. J. (1989): Propagation laws for the second-order moments of the Wigner distribution function in first-order optical systems, Optik 82, 173–181.

Bekshaev, A. Y., Soskin, M. S., Vasnetsov, M. V. (2003): Optical vortex symmetry breakdown and decomposition of the orbital angular momentum of light beams, J. Opt. Soc. Am. A 20, 1635–1643.

Born, M., Wolf, E. (1999): *Principles of Optics*, 7th ed. (Cambridge University Press, Cambridge).

Deng, D. M. (2006): Nonparaxial propagation of radially polarized light beams, J. Opt. Soc. Am. B 23, 1228–1234.

Encinas-Sanz, F., Serna, J., Martínez, C. Martínez-Herrero, R., Mejías, P. (1998): Time-varying beam quality factor and mode evolution TEA CO2 laser pulses, IEEE J. Quantum Electron., 34, 1835–1838.

Friberg, A. T. (1993): ed., *Selected Papers on Coherence and Radiometry* (SPIE Milestone Series, MS 69).

Giesen, A., Morin, M. (1998): eds., *Proceedings of the 4th International Workshop on Laser Beam and Optics Characterization* (LBOC4) (VDI-TechnologieZentrum, Munich).

Giesen, A., Weber, H. (2002): eds., *Proceedings of the 7th International Workshop on Laser Beam and Optics Characterization* (LBOC7) (Proc. SPIE 4932, Boulder, Colorado).

Gori, F., Bagini, V., Santarsiero, M., Frezza, F., Schettini, G., Schirripa Spagnolo, G. (1994): Coherent and partially coherent twisting beams, Opt. Rev. 1, 143–145.

Gori, F., Santarsiero, M., Piquero, G., Borghi, R., Mondello, A., Simon, R. (2001): Partially polarized Gaussian Schell-model beams, J. Opt. A Pure Appl. Opt. 3, 1–9.

Gori, F., Santarsiero, M., Borghi, R., Ramírez-Sánchez, V. (2008): Realizability condition for electromagnetic Schell-model sources, J. Opt. Soc. Am. A 25, 1016–1021.

Hodgson, H., Weber, H. (1993): Influence of spherical aberration of the active medium on the performance of Nd:YAG lasers**,** IEEE J. Quantum Electron. 29, 2497–2507.

ISO Standard 11146 (1999): Lasers and laser related equipment test methods for laser beams parameters: Beam widths, divergence angle and beam propagation factor.

ISO/DIS 12005 (2003): Optics and optical instruments-Lasers and laser related equipment-test methods for laser beam parameters: Polarization.

ISO 11146 (2005): Laser and laser related equipment-test methods for laser beam widths, divergence angles and beam propagation ratios, Parts 1, 2 and 3. International Organization for Standardization, Geneva, Switzerland.

Kudryashov, A. V., Paxton, A. H., Ilchenko, V. S., Giesen, A., Nickel, D., Davis, S. J., Heaven, M. C., Schriempf, J. T. (2006): eds., *Proceedings of the 8th International Workshop on Laser Beam and Optics Characterization* (LBOC8) (Proc. SPIE 6110, San Jose, CA).

Kuga, T., Torii, Y., Shiokawa, N., Hirano, T., Shimizu, Y., Sasada, H. (1997): Novel optical trap of atoms with a doughnut beam, Phys. Rew. Lett. 78, 4713–4716.

Kugler, N., Dong, N., Lü, Q., Weber, H. (1997): Investigation of the misalignment sensitivity of a birefringence: compensated two-rod Nd:YAG laser system, Appl. Opt. 36, 9359–9366.

Laabs, H., Weber, H. (2000): eds., *Proceedings of the 5th International Workshop on Laser Beam and Optics Characterization* (LBOC5) (VDI-TechnologieZentrum, Erice).

Lavi, S., Prochaska, R., Keren, E. (1988): Generalized beam parameters and transformation law for partially coherent light, Appl. Opt. 27, 3696–3703.

Lü, Q., Dong, S., Weber, H. (1995): Analysis of TEM_{00} laser beam quality degradation caused by a birefringent Nd:YAG rod, Opt. Quantum Electron. 27, 777–783.

Luo, S., Lu, B. (2003): M2 factor and kurtosis parameter of super-Gaussian beams passing through an axicon, Optik 114, 193–8.

Machavariani, G., Lumer, Y., Moshe, I., Jackel, S. (2007): Effect of the spiral phase element on the radial-polarization (0,1) * LG beam, Opt. Commun. 271, 190–196.

Mandel, L., Wolf, E. (1995): *Optical Coherence and Quantum Optics* (Cambridge University Press, Cambridge).

Marchand, E. W., Wolf, E. (1974): Walther′s definitions of generalized radiance, J. Opt. Soc. Am. 64(9), 1273–1274.

Martínez-Herrero, R., Mejías, P. M., Sánchez, M., Neira, J. L. H. (1992a): Third-and fourth-order parametric characterization of partially coherent beams propagating through ABCD optical systems, Opt. Quantum Electron. 24, 1021–1026.

Martínez-Herrero, R., Mejías, P. M., Piquero, G. (1992b): Quality improvement of partially coherent symmetric-intensity beams caused by quartic phase distorsions, Opt. Lett. 17, 1650–1651.

Martínez-Herrero, R., Mejías, P. M. (1993a): Quality improvement of symmetric-intensity beams propagating through pure phase plates, Opt. Commun. 95, 18–20.

Martínez-Herrero, R., Mejías, P. M. (1993b): Second-order spatial characterization of hard-edge diffracted beams, Opt. Lett. 18, 1669–1671.

Martínez-Herrero, R., Mejías, P. M. (1994): On the spatial parametric characterization of general light beams, *Current Trends in Optics*, Dainty, J. ed., Vol II (Academic Press, London, 105).

Martínez-Herrero, R., Piquero, G., Mejías, P. M. (1995a): On the propagation of the kurtosis parameter of general beams, Opt. Commun. 115, 225–232.

Martínez-Herrero, R., Mejías, P. M., Hodgson, N., Weber, H. (1995b): Beam-quality changes generated by thermally-induced spherical aberration in laser cavities, IEEE J. Quantum Electron. 31, 2173–2176.

Martínez-Herrero, R., Mejías, P. M., Arias, M. (1995c): Parametric characterization of coherent, lowest-order Gaussian beams propagating through hard-edge apertures, Opt. Lett. 20, 124–126.

Martínez-Herrero, R., Mejías, P. M. (1997a): On the fourth-order spatial characterization of laser beams: new invariant, Opt. Commun. 140, 57–60.

Martínez-Herrero, R., Mejías, P. M., Movilla, J. M. (1997b): Spatial characterization of partially polarized beams, Opt. Lett. 22, 206–208.

Martínez-Herrero, R., Mejías, P. M., Piquero, G. (2003a): Anisotropic pure-phase plates for quality improvement of partially coherent, partially polarized beams, J. Opt. Soc. Am. A 20, 577–581.

Martínez-Herrero, R., Mejías, P. M., Bosch, S., Carnicer, A. (2003b): Spatial width and power-content ratio of hard-edge diffracted beams, J. Opt. Soc. Am. A 20, 388–391.

Martínez-Herrero, R., Piquero, G., Mejías, P. M. (2004): Parametric characterization of the spatial structure of partially coherent and partially polarized beams, J. Opt. A: Pure Appl. Opt. 6, S67–S71.

Martínez-Herrero, R., Mejías, P. M., Movilla, J. M. (2005): Beam-quality optimization of partially polarized fields, J. Opt. Soc. Am. A 22, 1442–1446.

Martínez-Herrero, R., Mejías, P. M. (2006a): On the control of the spatial orientation of the transverse profile of a light beam, Opt. Express 14, 1086–1093.

Martínez-Herrero, R., Mejías, P. M. (2006b): On the spatial orientation of the transverse irradiance profile of partially coherent beams, Opt. Express 14, 3294–3303.

Martínez-Herrero, R., Mejías, P. M. (2007): Invariant parameters for characterizing nonuniformly partially polarized beams, Opt. Spectrosc. 103, 886–889.

Martínez-Herrero, R., Mejías, P. M., Piquero, G. (2008): Beam quality changes of radially and azimuthally polarized fields propagating through quartic phase, Opt. Commun. 281, 756–759.

Martínez-Herrero, R., Manjavacas, A. (2009): Overall second-order parametric characterization of light beams propagating through spiral phase elements, Opt. Commun. 282, 473–477.

McCelland, J. J., Scheinfein, M. R. J. (1991): Laser focusing of atoms: a particle-optics approach, J. Opt. Soc. Am. B 8, 1974–1986.

Mejías, P. M., Weber, H., Martínez-Herrero, R. (1993): González-Ureña, A., eds. *Proceedings of the 1st Workshop on Laser Beam Characterization* (LBOC1) (SEDO, Madrid).

Mejías, P. M., Martínez-Herrero, R. (1995): Time-resolved spatial parametric characterization of pulsed light beams, Opt. Lett. 20, 660–662.

Mejías, P. M., Martínez-Herrero, R., Piquero, G., Movilla, J. M. (2002): Parametric characterization of the spatial structure of non-uniformly polarizad laser beams, Prog. Quantum Electron. 26, 65–130.

Molina-Terriza, G., Rebane, L., Torres, J. P., Torner, L., Carrasco, S. (2007): Probing canonical geometrical objects by digital spiral Imaging, J. Eur. Opt. Soc. Rap. Public 2, 07014–07019.

Montmerle, B. A., Gilbert, M., Thro, P. Y., Weulersse, J. M. (2006): Thermal lensing and spherical aberration in high-power transversally pumped laser rods, Opt. Commun. 259, 223–235.

Morin, M., Giesen, A. (1996): eds., *Proceedings of the 3th International Workshop on Laser Beam Characterization* (LBOC3) (Proc. SPIE 2870, Quebec).
Movilla, J. M., Piquero, G., Martínez-Herrero, R., Mejías, P. M. (1998): Parametric characterization of non-uniformly polarized beams, Opt. Commun. 149, 230–234.
Movilla, J. M., Piquero, G., Martínez-Herrero, R., Mejías, P. M. (2000): On the measurement of the generalized degree of polarization, Opt. Quantum Electron. 32, 1333–1342.
Movilla, J. M., Martínez-Herrero, R., Mejías, P. M. (2001): Quality improvement of partially polarized beams, Appl. Opt. 40, 6098–6101.
Nemes, G., Siegman, A. E. (1994): Measurement of all ten second-order moments of an astigmatic beam by the use of rotating simple astigmatic (anamorphic) optics, J. Opt. Soc. Am. A 11, 2257–2264.
Niv, A., Biener, G., Kleiner, V., Hasman, E. (2005): Spiral phase elements obtained by use of discrete space-variant subwavelength gratings, Opt.Commun. 251, 306–314.
Oemrawsingh, S. S. R.; van Houwelingen, J. A. W.; Eliel, E. R., Woerdman, J. P., Verstegen, E. J. K., Kloosterboer, J. G., Hooft, G. W. (2004): Production and characterization of spiral phase plates for optical wavelengths, Appl. Opt. 43, 688–694.
Oron, R., Davidson, N., Friesem, A. A., Hasman, E. (2002): Continuous-phase elements can improve laser beam quality, Opt. Lett. 25, 939–941.
Pepper, D. M. (1985): Nonlinear optical phase conjugation, *Laser Handbook*, M. L. Stitch, M. L., and M. Bass, M., eds., Vol 4 (North-Holland, Amsterdam, 433–485).
Perina, J. (1971): *Coherence of Light* (Van Nostrand Reinhold Company, London).
Piquero, G., Mejías, P. M., Martínez-Herrero, R. (1994): Sharpness changes of Gaussian beams induced by spherically aberrated lenses, Opt. Commun. 107, 179–183.
Piquero, G., Gori, F., Romanini, P., Santarsiero, M., Borghi, R., Mondello, A. (2002): Synthesis of partially polarized Gaussian Schell-model sources, Opt. Commun. 208, 9–16.
Ramírez-Sánchez, V., Piquero, G. (2006): Global beam shaping with non-uniformly polarized beams: a proposal, Appl. Opt. 45, 8902–8906.
Sato, S., Harada, Y., Waseda, Y. (1994): Optical trapping of microscopic metal particles, Opt. Lett. 19, 1807–1809.
Serna, J., Martínez-Herrero, R., Mejías, P. M. (1991): Parametric characterization of general partially coherent beams propagating through ABCD optical systems, J. Opt. Soc. Am. A 8, 1094–1098.
Serna, J., Mejías, P. M., Martínez-Herrero, R. (1992a): Rotation of partially coherent beams propagating through free space, Opt. Quantum Electron. 24, S873–S880.
Serna, J., Mejías, P. M., Martínez-Herrero, R. (1992b): Beam quality changes of Gaussian Schell-model fields propagating through Gaussian apertures, Appl. Opt. 31, 4330–4331.
Siegman, A. E. (1986): *Lasers*, (University Science Books, California).
Siegman, A. E. (1990): New developments in laser resonators, *Optical Resonators*, Holmes, D. A., ed., Proc. SPIE, Vol1224, 2–14.
Siegman, A. E. (1993a): Analysis of laser beam quality degradation caused by spherical aberration, Appl. Opt. 32, 5893–5901.
Siegman, A. E. (1993b): Binary phase plates cannot improve laser beam quality, Opt. Lett. 18, 675–677.
Simon, R, Mukunda, N., Sudarshan, E. C. G. (1988): Partially coherent beams and a generalized ABCD-law, Opt. Commun. 65, 322–328.
Simon, R., Mukunda, N. (1993): Twisted Gaussian-Schell-model beams, J. Opt. Soc. Am. A 10, 95–109.
Torner, L., Torres, J., Carrasco, S. (2005): Digital spiral imaging, Opt. Express 13, 873–881.
Vasnetsov, M. V., Torres, J. P., Petrov, D. V., Torner, L. (2003): Observation of the orbital angular momentum spectrum of a light beam, Opt. Lett. 28, 2285–2287.
Walther, A. (1968): Radiometry and coherence, J. Opt. Soc. Am. 58, 1256–1259.
Weber, H. (1992): Propagation of higher-order intensity moments in quadratic-index media, Opt. Quantum Electron. 24, 1027–1049.

Weber, H., Reng, N., Lüdtke, J., Mejías, P. M. (1994): eds., *Proceedings of the 2nd Workshop on Laser Beam Characterization* (LBOC2) (FLI, Berlín).

WLT (2001): eds., *Proceedings of the 6th International Workshop on Laser Beam and Optics Characterization* (LBOC6) (WLT, Munich).

Wolf, E. (2007): *Introduction to the Theory of Coherence and Polarization of Light* (Cambridge University Press, Cambridge).

Xie, Q., Zhao, D. (2008): Optical vortices generated by multi-level achromatic spiral phase plates for broadband beams, Opt. Commun. 281, 7–11.

Zhou, G. Q. (2006): Analytical vectorial structure of Laguerre-Gaussian beam in the far field, Opt. Lett. 31, 2616–2618.

http://www.springer.com/978-3-642-01326-3

Characterization of Partially Polarized Light Fields
Martínez-Herrero, R.; Mejías, P.M.; Piquero, G.
2009, XIII, 179 p. 60 illus., Hardcover
ISBN: 978-3-642-01326-3